

Hierarchical Riesz Bases for $H^s(\Omega)$, $1 < s < \frac{5}{2}$

Oleg Davydov and Rob Stevenson

January 10, 2005

Abstract

On arbitrary polygonal domains $\Omega \subset \mathbb{R}^2$, we construct C^1 hierarchical Riesz bases for Sobolev spaces $H^s(\Omega)$. In contrast to an earlier construction by Dahmen, Oswald and Shi ([5]), our bases will be of Lagrange instead of Hermite type, by which we extend the range of stability from $s \in (2, \frac{5}{2})$ to $s \in (1, \frac{5}{2})$. Since the latter range includes $s = 2$, with respect to the present basis, the stiffness matrices of fourth order elliptic problems are uniformly well-conditioned.

2000 *Mathematics Subject Classification.* 41A15, 65D07, 65T60, 65N30, 41A63.

Key words and phrases. Hierarchical bases, splines, C^1 finite elements

1 Introduction

This paper deals with the construction of Riesz bases for the Sobolev spaces $H^s(\Omega)$ for $s \in (1, \frac{5}{2})$ on arbitrary polygonal domains $\Omega \subset \mathbb{R}^2$. Because of the generally non-trivial geometry of Ω , as well as in view of an efficient implementation, one has to employ *multiscale bases*. Starting with a nested sequence of approximation spaces, the idea of such bases is to construct them recursively by adding to the basis from the previous approximation space a set of locally supported functions spanning a complement space such that the union is a basis of the current approximation space. In particular, we will use *hierarchical bases* meaning that the functions that are added are just

a subset of a *single-scale basis* for the space on the current level. Since such functions do not have zero mean, the resulting infinite collection may only yield a basis for $H^s(\Omega)$ for positive s .

In case the functions that are added from level to level do have vanishing moments, *i.e.*, their integrals against all polynomials up to a certain degree vanish, we speak about *wavelet bases*. Several wavelet constructions on polygonal domains are known that generate Riesz bases for $H^s(\Omega)$ for s in a range around zero (see *e.g.* [6, 8, 15]). With most constructions, at least a subset of the wavelets are only continuous, so that the range of stability is restricted to $s < \frac{3}{2}$. In particular, the only available wavelet type Riesz basis for $H^s(\Omega)$ and $s > \frac{3}{2}$ on general polygons is that of [7], which is based on domain decomposition and employs a Hestenes extension operator.

Hierarchical bases were constructed first in [24], based on C^0 finite elements. For domains in \mathbb{R}^2 they give rise to Riesz bases for $H^s(\Omega)$, $s \in (1, \frac{3}{2})$, with a suboptimal result (leading to logarithmically growing condition numbers of related stiffness matrices) in the case $s = 1$ most interesting for practice. For $s \geq \frac{3}{2}$, C^1 piecewise polynomials can be used as shown in [22] and [5], where hierarchical bases are constructed that are Riesz bases for $s \in (2, \frac{5}{2})$. In [12] these bases are employed for surface compression. Instead of the classical Hermite type finite element bases used in [5, 12, 22], in this paper we employ single scale bases of Lagrange type, which allows us to enlarge the range of stability of the resulting hierarchical basis to $s \in (1, \frac{5}{2})$, which thus safely includes the value $s = 2$ important for the application to solving the biharmonic equation.

The approximation spaces used in our construction are the spaces of C^1 piecewise cubic polynomials on certain special triangulations (see Section 2 for their description) which are available for any polygonal domain, as shown in Appendix A. On domains that allow a conforming quadrangulation with all interior vertices of degree four, these triangulations are the standard triangulated quadrangulations (so called *FVS triangulations*) associated with the well known Fraeijs de Veubeke-Sander quadrilateral C^1 cubic finite elements. Recently, locally supported Lagrange bases for the spaces of C^1 piecewise cubic polynomials on FVS triangulations have appeared in [18, 19, 20].

An important property of FVS triangulations is that they can be regularly refined leading to a nested sequence of approximation spaces, see *e.g.* [5, 13]. Although the single scale Lagrange bases corresponding to each level of refinement are not stable with respect to the metric of $H^s(\Omega)$, $s > 0$, they can be employed to construct hierarchical Riesz bases for Sobolev spaces if they

are L_2 -stable and if the Lagrange interpolation sets of consecutive refinement levels are *nested*. To ensure this last property we restrict ourselves to the so called *checkerboard triangulations* [18], and replace the standard dyadic refinement with a *triadic* one. Since many important domains (e.g. a triangle) do not allow a checkerboard triangulation, we use a slightly wider class of triangulations which can be employed on any polygon, and at the same time results in nested spaces.

The starting point for our construction in this paper is the Lagrange basis for C^1 piecewise cubics mentioned in [9, Remark 2.5], which is related to the Bernstein-Bézier basis used in [9] to define a scattered data fitting method. However, as we will see, aiming at constructing hierarchical Lagrange bases we have to modify the construction from [9]. The technically most difficult part is to find correct constellations of the interpolation points near the domain boundary preserving all required properties such as locality and stability of the basis functions and nesting of the interpolation sets.

The paper is organized as follows.

In Section 2, the nested sequence of C^1 piecewise cubic approximation spaces is defined with respect to increasingly finer subdivisions by triadic refinements of the two-dimensional domain into quadrilaterals generally augmented by triangles at the boundary. Precise conditions on the initial subdivision are formulated, which, as in shown in Appendix A, can be fulfilled for any polygon.

In Section 3, after deriving some auxiliary results concerning the stability of local interpolation problems, we give a formula for the dimension of the approximation spaces.

In Section 4, locally supported, single scale Lagrange bases are constructed, and their uniform L_2 -stability is proven.

Finally, in Sections 5 and 6, the theory of multiscale decompositions is applied to show that the above Lagrange bases give rise to a hierarchical basis which, properly scaled, yields a Riesz basis for $H^s(\Omega)$, $1 < s < \frac{5}{2}$.

In order to avoid the repeated use of generic but unspecified constants, in this paper by $C \lesssim D$ we mean that C can be bounded by a multiple of D , independently of parameters which C and D may depend on. Furthermore, $C \gtrsim D$ is defined as $D \lesssim C$, and $C \approx D$ as “ $C \lesssim D$ and $C \gtrsim D$.”

2 Multilevel spaces of C^1 piecewise cubics

Let $\Omega \subset \mathbb{R}^2$ be a domain for which there is a collection \diamond_0 of (closed) convex nondegenerate quadrilaterals such that

- (a) $\Omega \subset \cup_{Q \in \diamond_0} Q$,
- (b) The intersection of any two different quadrilaterals from \diamond_0 is either empty or a common edge or vertex.
- (c)
 - All interior vertices are of degree four,
 - the edges of all quadrilaterals can be given predicates north, east, south, and west in clockwise direction such that different quadrilaterals may only share north-south or east-west edges, and
 - \diamond_0 allows a splitting into disjoint subsets \diamond_0^\bullet and \diamond_0° of black and white quadrilaterals such that each quadrilateral shares its edges only with quadrilaterals of opposite color.
- (d) Each $Q \in \diamond_0$ has non-empty intersection with Ω , and if $\text{int}(Q) \not\subset \Omega$, then one of the diagonals of Q is on $\partial\Omega$. We set

$$\partial\diamond_0 = \{Q \in \diamond_0 : \text{int}(Q) \not\subset \Omega\}.$$

In addition, we assume that one of both triangles defined by cutting $Q \in \partial\diamond_0$ along $\partial\Omega$ is inside $\overline{\Omega}$ and the other one is outside Ω .

- (e) Different $Q, Q' \in \partial\diamond_0$ do not share an edge.

Note that Ω has a polygonal boundary. An illustration is given in Figure 1.

At a first glance the assumptions (a)–(e) may look very restrictive. However, as we will show in Appendix A, a quadrangulation of this type can be constructed for any domain with Lipschitz' continuous, piecewise linear boundary (also non-convex and multiply connected).

Remark 2.1. Allowing multiply connected domains, none of the conditions in (c) is implied by two others.

Remark 2.2. The conditions (a)–(c) are very similar to those imposed in [18] on what is called there being a checkerboard quadrangulation, except that no triangles at the boundary are allowed there, i.e., $\partial\diamond_0 = \emptyset$. The possible presence of triangles at the boundary will rather complicate our

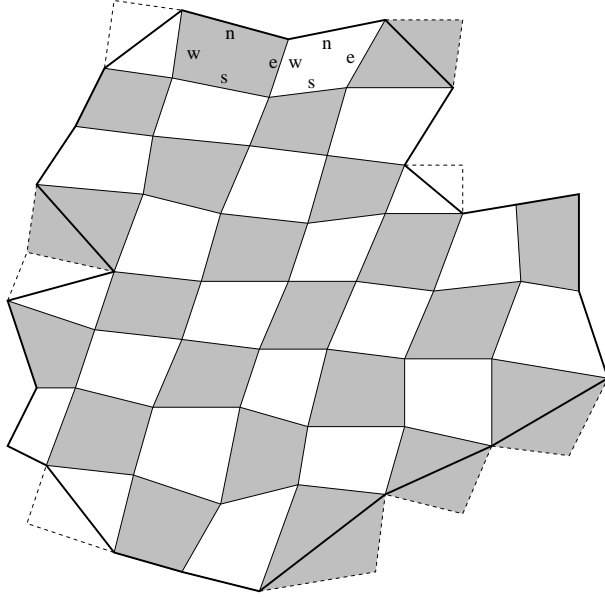


Figure 1: Polygonal domain and a quadrangulation \diamond_0 .

task of constructing a suitable hierarchical basis. On the other hand, they allow us to treat general polygons. Indeed, a simple argument involving the degrees of the boundary vertices shows that without allowing triangles at the boundary, a quadrangulation satisfying (a)–(c) of e.g. any triangular domain does not exist.

Let Δ_0 be the triangulation of Ω obtained by adding both diagonals to each quadrilateral $Q \in \diamond_0$, as in [18], and by removing all the resulting triangles not lying in $\overline{\Omega}$ (cf. Figure 7).

Remark 2.3. Although (a)–(e) do permit quadrangulations of domains having cracks, for those domains some conditions are unnecessarily restrictive. All restrictions induced by (a)–(e) on relations between triangles from Δ_0 on both sides of a crack are actually irrelevant. For example, it does not matter when such triangles have partly overlapping edges. Although, for ease of presentation, we assumed that one of both triangles defined by cutting $Q \in \partial \diamond_0$ along $\partial \Omega$ is inside $\overline{\Omega}$ and the other one is outside Ω , one may keep in mind that the latter triangle is actually a virtual one since it does not belong to the triangulation Δ_0 which will be used to define the spaces of piecewise

cubics. So in particular it does not matter that for domains with cracks it cannot always be avoided that such virtual triangles do intersect with Ω .

By subdividing each quadrilateral in \diamond_0 into 9 subquadrilaterals as indicated in Figure 2, we arrive at a refined quadrangulation \diamond_1 . As \diamond_0 gave rise to \triangle_0 , \diamond_1 gives rise to a triangulation \triangle_1 , which is a refinement of \triangle_0 . The coloring of the quadrilaterals from \diamond_0 and the labeling of their edges induces a coloring and labeling for quadrilaterals from \diamond_1 as is also indicated in Figure 2.

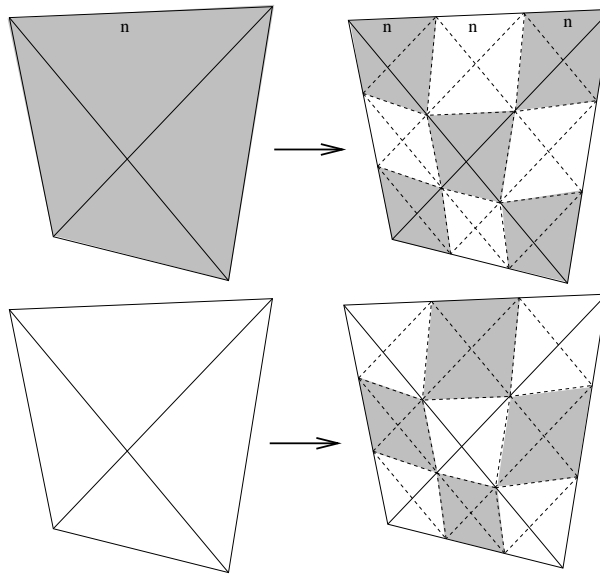


Figure 2: Refinement of a quadrilateral, and the induced coloring and edge labeling of the new quadrilaterals.

Repeating this process, we get a sequence of successively refined quadrangulations

$$\diamond_0, \diamond_1, \dots, \diamond_n, \dots,$$

and triangulations

$$\triangle_0, \triangle_1, \dots, \triangle_n, \dots$$

All quadrangulations \diamond_n satisfy the properties (a)–(e) that were listed for \diamond_0 . As for $n = 0$ above, we denote by $\partial\diamond_n$ the subset of \diamond_n of those quadrilaterals

$Q \in \diamond_n$ having interiors that are not completely contained in Ω , and by \diamond_n^\bullet and \diamond_n° we denote the sets of black and white quadrilaterals in \diamond_n .

Similar to [5, Proposition 5.2], it can be verified that each quadrilateral from \diamond_2 is either a parallelogram or geometrically similar to a quadrilateral from \diamond_1 . As a consequence, all quadrilaterals generated in subsequent subdivisions are similar to quadrilaterals in \diamond_1 or \diamond_2 , and so we infer that the smallest angle of any triangle in all triangulations Δ_n , $n = 0, 1, \dots$, is bounded from below by some positive constant

θ .

In order not to be forced to handle many exceptional cases in §4, in addition to (a)-(e), we assume that all \diamond_n satisfy the following condition:

- (f) – No $Q \in \diamond_n \setminus \partial \diamond_n$ shares two opposite edges with quadrilaterals in $\partial \diamond_n$.
- If $v \notin \partial \Omega$ is a vertex of $Q \in \partial \diamond_n$, then v is shared by three quadrilaterals in $\diamond_n \setminus \partial \diamond_n$, with one of them having no common edges with quadrilaterals in $\partial \diamond_n$.

One easily verifies that if \diamond_0 satisfies (a)–(f), then all \diamond_n satisfy (a)–(f). Moreover, in particular because of (e), if \diamond_0 satisfies (a)–(e), then \diamond_1 , and thus \diamond_n for all $n \geq 1$ satisfy (a)–(f). So possibly by replacing the initial quadrangulation \diamond_0 by \diamond_1 we may always assume that (f) is valid. Note that in practice (f) can be achieved using a much more moderate refinement of \diamond_0 . In particular, a *dyadic* refinement always suffices.

For each $n = 0, 1, \dots$, we consider the space \mathcal{S}_n of cubic piecewise polynomials with respect to Δ_n satisfying the homogeneous boundary conditions, *i.e.*,

$$\mathcal{S}_n = \{s \in C^1(\Omega) : s|_T \in \mathcal{P}_3 \text{ for all } T \in \Delta_n, \text{ and } s = \frac{\partial s}{\partial x} = \frac{\partial s}{\partial y} = 0 \text{ on } \partial \Omega\},$$

where \mathcal{P}_3 is the space of all bivariate polynomials of total degree at most 3.

It is clear that the spaces \mathcal{S}_n are *nested*, *i.e.*,

$$\mathcal{S}_0 \subset \mathcal{S}_1 \subset \dots \subset \mathcal{S}_n \subset \dots \tag{2.1}$$

3 Dimension of \mathcal{S}_n

As a preparation for the construction of a basis, we compute the dimension of \mathcal{S}_n . We start with three lemmas that will also be used in the next section. Note that we use *nodal smoothness conditions* (see e.g. [10, 17]) in the proofs although the *Bernstein-Bézier techniques* employed in [18]–[20] and [9] could have been applied with equal success. In the figures below we employ usual symbols (dots, circles and arrows) to indicate nodal degrees of freedom (see [2]).

An important tool repeatedly used in this section is the classical *Markov inequality*

$$\|p'\|_{L_\infty(0,1)} \leq 2q^2 \|p\|_{L_\infty(0,1)}$$

valid for any univariate polynomial p of degree q . We often apply this inequality in the following form: Let e be a line segment in \mathbb{R}^2 with endpoints v and w , and let s be a bivariate polynomial of total degree q . With $\frac{\partial s}{\partial e}(v)$ we denote the derivative of s at v in the direction $w - v$. Defining $p(t) = s(v + t(w - v))$, we have $\frac{\partial s}{\partial e}(v) = \frac{p'(0)}{|e|}$, and Markov's inequality shows that

$$\left| \frac{\partial s}{\partial e}(v) \right| \leq \frac{2q^2}{|e|} \|s\|_{L_\infty(e)}.$$

Lemma 3.1. *Let T be a triangle with vertices v_1, v_2, v_3 , see Figure 3. Denote by w the midpoint of the edge e connecting v_2 and v_3 , and by h the diameter of T . Then for every cubic polynomial $s \in \mathcal{P}_3$ we have*

$$\|s\|_{L_\infty(T)} \lesssim \max \left\{ |s(v_i)|, h \left| \frac{\partial s}{\partial x}(v_i) \right|, h \left| \frac{\partial s}{\partial y}(v_i) \right|, 1 \leq i \leq 3, h \left| \frac{\partial s}{\partial e^\perp}(w) \right| \right\}, \quad (3.1)$$

with a constant depending only on the smallest angle in T . Moreover, for any $a \in \mathbb{R}^{10}$ there exists a unique $s \in \mathcal{P}_3$ such that the ten functionals that determine the right hand side of (3.1) have the values a_1 to a_{10} .

Proof. Without loss of generality we may assume that v_1 is located at the origin of the coordinate system. Moreover, a simple scaling argument shows that it is sufficient to prove (3.1) for triangles T with diameter $h = 1$ and polynomials $s \in \mathcal{P}_3$ with $\|s\|_{L_\infty(T)} = 1$. For any fixed $\gamma > 0$, the set of all such triangle/polynomial pairs (each identified with a point in \mathbb{R}^{14} representing the four coordinates of v_2, v_3 and ten coefficients of s with respect to a fixed polynomial basis), such that the minimal angle of the triangle is at least

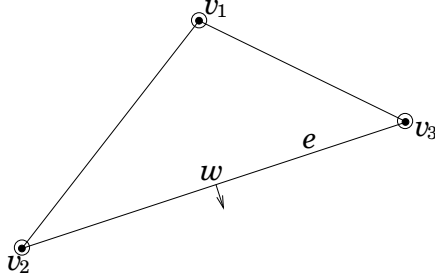


Figure 3: Triangle T , and degrees of freedom corresponding to Lemma 3.1.

γ , is compact. Therefore, the right hand side of (3.1) (with $h = 1$), as a continuous function on this compact set, attains its minimum value μ for a triangle T and a polynomial s . If $\mu > 0$, then its reciprocal is the desired constant in (3.1). Since μ is obviously nonnegative, it remains to show that μ cannot be zero.

Let us assume that $\mu = 0$. Then all values

$$s(v_i), \frac{\partial s}{\partial x}(v_i), \frac{\partial s}{\partial y}(v_i), \quad 1 \leq i \leq 3, \quad \frac{\partial s}{\partial e^\perp}(w) \quad (3.2)$$

are zero. Because of its vanishing function value and first order derivative at both endpoints, the univariate cubic polynomial $s|_e$ is zero. Because of its vanishing function value at both endpoints and at the midpoint, also the univariate quadratic polynomial $\frac{\partial s}{\partial e^\perp}|_e$ is zero. Now let $z \neq v_1$ be any point in T , and let ℓ be the straight line through z and v_1 . Since both its function value and first order derivative vanish at both v_1 and at the intersection point of ℓ and e , the univariate cubic polynomial $s|_\ell$ is zero, and so $s(z) = 0$, or $s = 0$, in contradiction to the assumption $\|s\|_{L^\infty(T)} = 1$.

This last argument also shows that the ten nodal functionals from (3.2) span $(\mathcal{P}_3)^*$. (As usual, we denote by X^* the dual space of a linear space X .) Since $\dim(\mathcal{P}_3) = 10$, they do not only span $(\mathcal{P}_3)^*$, but necessarily generate a basis for it, which proves the last statement of the lemma. \square

Lemma 3.2. *Let T_1, T_2 be two triangles with vertices v, v_1, v_2 and v, v_2, v_3 , respectively, see Figure 4. With α_1, α_2 being the angles of T_1, T_2 at v_2 , we assume that $\alpha_1 + \alpha_2 \neq \pi$. Let w_1 and w_2 be the midpoints of the edges $[v_1, v_2]$ and $[v_2, v_3]$, respectively. We denote by h the diameter of $T_1 \cup T_2$, and by e*

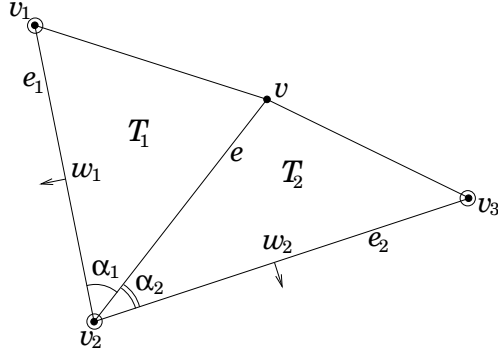


Figure 4: Illustration to Lemma 3.2.

the edge $T_1 \cap T_2$. Then for any C^1 cubic piecewise polynomial s with respect to the pair of triangles T_1, T_2 we have

$$\|s|_e\|_{L_\infty(e)} \lesssim \max \left\{ |s(v_i)|, h \left| \frac{\partial s}{\partial x}(v_i) \right|, h \left| \frac{\partial s}{\partial y}(v_i) \right|, i = 1, 2, 3, \right. \\ \left. h \left| \frac{\partial s}{\partial e_i^\perp}(w_i) \right|, i = 1, 2, |s(v)| \right\}, \quad (3.3)$$

with a constant depending only on the smallest angle γ from T_1, T_2 and on $|\pi - (\alpha_1 + \alpha_2)|$. If $[v_1, v] \cup [v, v_3]$ is a straight line, then $\pi - (\alpha_1 + \alpha_2)$ has a positive lower bound in terms of the smallest angle from T_1 and T_2 , and the constant in (3.3) depends only on γ .

Proof. Let $e_1 = [v_2, v_1]$, $e_2 = [v_2, v_3]$ and $e = [v_2, v]$. Since a univariate cubic polynomial is uniquely determined by its function and first derivative values at the endpoints of an interval, we have

$$\|s|_{e_i}\|_{L_\infty(e_i)} \lesssim \max \left\{ |s(v_j)|, h \left| \frac{\partial s}{\partial x}(v_j) \right|, h \left| \frac{\partial s}{\partial y}(v_j) \right|, j = i, i + 1 \right\}, \quad i = 1, 2.$$

Similarly, since a univariate quadratic polynomial is uniquely determined by its values at the endpoints and at the middle point of an interval, it follows that

$$\left\| \frac{\partial s}{\partial e_i^\perp} |_{e_i} \right\|_{L_\infty(e_i)} \lesssim \max \left\{ \left| \frac{\partial s}{\partial x}(v_j) \right|, \left| \frac{\partial s}{\partial y}(v_j) \right|, j = i, i + 1, \left| \frac{\partial s}{\partial e_i^\perp}(w_i) \right| \right\}, \quad i = 1, 2.$$

Since

$$\begin{aligned}\frac{\partial^2}{\partial e \partial e_i}(s|_{T_i})(v_2) &= \frac{\partial}{\partial e_i} \left(\cos \alpha_i \frac{\partial}{\partial e_i}(s|_{T_i}) \pm \sin \alpha_i \frac{\partial}{\partial e_i^\perp}(s|_{T_i}) \right)(v_2) \\ &= \cos \alpha_i \frac{\partial^2}{\partial e_i^2}(s|_{T_i})(v_2) \pm \sin \alpha_i \frac{\partial^2}{\partial e_i \partial e_i^\perp}(s|_{T_i})(v_2)\end{aligned}$$

(where the choice of “+” or “−” depends on the orientation of e_i^\perp and has no influence on our argumentation), we conclude by Markov’s inequality that

$$h^2 \left| \frac{\partial^2}{\partial e \partial e_i}(s|_{T_i})(v_2) \right| \lesssim M, \quad i = 1, 2,$$

with

$$M := \max \left\{ |s(v_i)|, h \left| \frac{\partial s}{\partial x}(v_i) \right|, h \left| \frac{\partial s}{\partial y}(v_i) \right|, i = 1, 2, 3, h \left| \frac{\partial s}{\partial e_i^\perp}(w_i) \right|, i = 1, 2 \right\}.$$

Now, since s is C^1 across the edge e , we have by a nodal smoothness condition [17, formula (II)],

$$\frac{\partial^2}{\partial e^2}(s|_e)(v_2) \sin(\alpha_1 + \alpha_2) = \frac{\partial^2}{\partial e \partial e_1}(s|_{T_1})(v_2) \sin \alpha_2 + \frac{\partial^2}{\partial e \partial e_2}(s|_{T_2})(v_2) \sin \alpha_1,$$

which implies

$$h^2 \left| \frac{\partial^2}{\partial e^2}(s|_e)(v_2) \right| \lesssim M / |\pi - (\alpha_1 + \alpha_2)|.$$

Taking into account also the inequality

$$\left| \frac{\partial s}{\partial e}(v_2) \right| \lesssim \max \left\{ \left| \frac{\partial s}{\partial x}(v_2) \right|, \left| \frac{\partial s}{\partial y}(v_2) \right| \right\}$$

and the fact that a univariate cubic polynomial is uniquely determined by its function values at the endpoints of an interval and first and second derivatives at one endpoint, we arrive at the estimate

$$\begin{aligned}\|s|_e\|_{L_\infty(e)} &\lesssim \max \left\{ |s(v_2)|, h \left| \frac{\partial s}{\partial e}(v_2) \right|, h^2 \left| \frac{\partial^2}{\partial e^2}(s|_e)(v_2) \right|, |s(v)| \right\} \\ &\lesssim \max \left\{ |s(v)|, M / |\pi - (\alpha_1 + \alpha_2)| \right\},\end{aligned}$$

which completes the proof of (3.3).

The final statement of the lemma is obvious. Note that in our applications of this lemma, $[v_1, v] \cup [v, v_3]$ will always be a straight line. \square

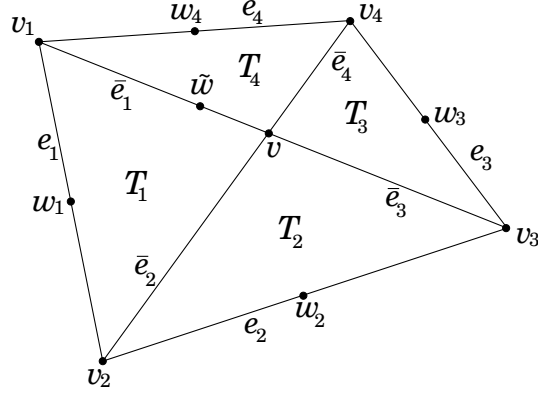


Figure 5: Quadrilateral Q of Lemma 3.3.

Lemma 3.3. *Let Q be a convex nondegenerate quadrilateral with vertices v_1, \dots, v_4 numbered in counterclockwise direction, and edges $e_1 = [v_1, v_2]$, $e_2 = [v_2, v_3]$, $e_3 = [v_3, v_4]$ and $e_4 = [v_4, v_1]$, see Figure 5. We denote by w_i the midpoint of e_i and by v the intersection point of the diagonals of Q , and set $\tilde{w} = \frac{2}{3}v + \frac{1}{3}v_1$ and $\bar{e}_i = [v_i, v]$. Let Δ_Q denote the triangulation of Q into four triangles T_1, \dots, T_4 obtained by splitting Q along both its diagonals, where e_i is an edge of T_i , and denote by h the diameter of Q . Then for any C^1 cubic piecewise polynomial s with respect to Δ_Q , we have*

$$\|s\|_{L_\infty(Q)} \lesssim \max \left\{ |s(v_i)|, h \left| \frac{\partial s}{\partial x}(v_i) \right|, h \left| \frac{\partial s}{\partial y}(v_i) \right|, h \left| \frac{\partial s}{\partial e_i^\perp}(w_i) \right|, 1 \leq i \leq 4 \right\}, \quad (3.4)$$

$$\|s\|_{L_\infty(Q)} \lesssim \max \left\{ |s(v_i)|, h \left| \frac{\partial s}{\partial x}(v_i) \right|, h \left| \frac{\partial s}{\partial y}(v_i) \right|, i = 1, \dots, 4, \right. \\ \left. h \left| \frac{\partial s}{\partial e_i^\perp}(w_i) \right|, i = 1, 2, |s(v)|, |s(\tilde{w})| \right\}, \quad (3.5)$$

$$\|s\|_{L_\infty(Q)} \lesssim \max \left\{ |s(v_i)|, h \left| \frac{\partial s}{\partial x}(v_i) \right|, h \left| \frac{\partial s}{\partial y}(v_i) \right|, i = 1, \dots, 4, \right. \\ \left. h \left| \frac{\partial s}{\partial e_i^\perp}(w_i) \right|, i = 1, 2, 3, |s(v)| \right\}, \quad (3.6)$$

and

$$\|s\|_{L_\infty(Q)} \lesssim \max \left\{ |s(v_i)|, h \left| \frac{\partial s}{\partial x}(v_i) \right|, h \left| \frac{\partial s}{\partial y}(v_i) \right|, i = 1, \dots, 4, \right. \\ \left. h \left| \frac{\partial s}{\partial e_i^\perp}(w_i) \right|, i = 1, 3, |s(v)|, |s(\tilde{w})| \right\}, \quad (3.7)$$

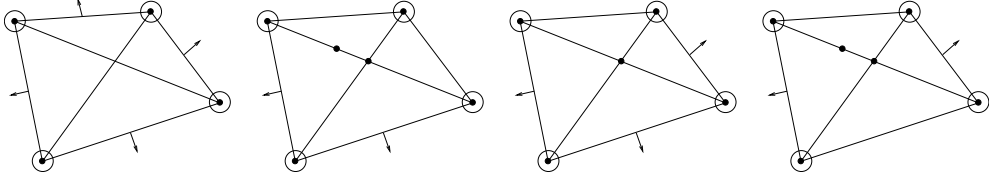


Figure 6: Degrees of freedom corresponding to (3.4), (3.5), (3.6) and (3.7).

with constants depending only on the smallest angle in Δ_Q , cf. Figure 6. Moreover, for any $a \in \mathbb{R}^{16}$, there exists a unique C^1 cubic piecewise polynomial with respect to Δ_Q such that the sixteen functionals that determine the right hand side of either (3.4), (3.5), (3.6) or (3.7) have the values a_1 to a_{16} .

Proof. The estimate (3.4) together with the last statement for this set of functionals follows immediately from the standard theory of the Fraeijs de Veubeke-Sander finite element (see, e.g. [2]).

To show (3.5), we first apply Lemma 3.2 to the triangles T_1, T_2 , which shows that

$$\|s|_{\bar{e}_2}\|_{L_\infty(\bar{e}_2)} \lesssim M,$$

where M is the right hand side of (3.5). From this we find

$$h \left| \frac{\partial s}{\partial \bar{e}_2}(v) \right| \lesssim M.$$

In addition, by considering a univariate cubic polynomial obtained by restricting s to the edge \bar{e}_1 , we conclude that

$$h \left| \frac{\partial s}{\partial \bar{e}_1}(v) \right| \lesssim \max \left\{ |s(v_1)|, h \left| \frac{\partial s}{\partial \bar{e}_1}(v_1) \right|, |s(\tilde{w})|, |s(v)| \right\} \lesssim M.$$

Therefore,

$$\max \left\{ h \left| \frac{\partial s}{\partial x}(v) \right|, h \left| \frac{\partial s}{\partial y}(v) \right| \right\} \lesssim M, \quad (3.8)$$

and Lemma 3.1 shows that $\|s\|_{L_\infty(T_1 \cup T_2)} \lesssim M$. In particular, the univariate cubic polynomials obtained by restricting s to the intervals \bar{e}_1 , $[w_1, \frac{1}{2}v + \frac{1}{2}v_1]$, \bar{e}_3 and $[w_2, \frac{1}{2}v + \frac{1}{2}v_3]$ are bounded by M multiplied with a constant depending only on the smallest angle in Δ_Q . By Markov's inequality it then follows that

$$\max \left\{ h \left| \frac{\partial s}{\partial \bar{e}_1}(\frac{1}{2}v + \frac{1}{2}v_1) \right|, h \left| \frac{\partial s}{\partial \bar{e}_3}(\frac{1}{2}v + \frac{1}{2}v_3) \right| \right\} \lesssim M,$$

which allows to apply Lemma 3.1 also to T_3, T_4 completing the proof of (3.5).

The proof of (3.6) is quite similar to the above proof of (3.5), where the only difference is that (3.8), with M now being the right hand side of (3.6), is obtained by applying Lemma 3.2 twice, namely to the pairs of triangles T_1, T_2 and T_2, T_3 .

Next, we prove (3.7). By a well-known interpolation scheme for univariate cubic polynomials,

$$\|s|_{\bar{e}_1}\|_{L_\infty(\bar{e}_1)} \lesssim \max \left\{ |s(v_1)|, h \left| \frac{\partial s}{\partial \bar{e}_1}(v_1) \right|, |s(v)|, |s(\tilde{w})| \right\} \lesssim M, \quad (3.9)$$

where M denotes the right hand side of (3.7) this time. Furthermore, as in the beginning of the proof of Lemma 3.2, we get

$$\begin{aligned} h^2 \left| \frac{\partial^2}{\partial \bar{e}_1 \partial e_1}(s|_{T_1})(v_1) \right| &\lesssim \max \left\{ |s(v_i)|, h \left| \frac{\partial s}{\partial x}(v_i) \right|, h \left| \frac{\partial s}{\partial y}(v_i) \right|, i = 1, 2, h \left| \frac{\partial s}{\partial e_1^\perp}(w_1) \right| \right\} \\ &\lesssim M. \end{aligned}$$

Using the C^1 -smoothness across \bar{e}_1 , we have

$$\frac{\partial^2}{\partial \bar{e}_1 \partial e_4}(s|_{T_4})(v_1) \sin \alpha_1 = \frac{\partial^2}{\partial \bar{e}_1 \partial e_1}(s|_{T_1})(v_1) \sin \alpha_2 - \frac{\partial^2}{\partial \bar{e}_1^2}(s|_{\bar{e}_1})(v_1) \sin(\alpha_1 + \alpha_2),$$

where α_1, α_2 are the angles of T_1 , respectively T_4 , at v_1 . Since also

$$\|s|_{e_4}\|_{L_\infty(e_4)} \lesssim \max \left\{ |s(v_i)|, h \left| \frac{\partial s}{\partial x}(v_i) \right|, h \left| \frac{\partial s}{\partial y}(v_i) \right|, i = 1, 4 \right\},$$

it follows that

$$h^2 \left| \frac{\partial^2}{\partial e_4 \partial e_4^\perp}(s|_{T_4})(v_1) \right| = h^2 \left| \frac{\partial^2}{\partial \bar{e}_1 \partial e_4}(s|_{T_4})(v_1) + \frac{\partial^2}{\partial \bar{e}_1^2}(s|_{T_4})(v_1) \cos \alpha_2 \right| / \sin \alpha_2 \lesssim M.$$

By a univariate quadratic interpolation scheme, we get

$$\left\| \frac{\partial s}{\partial e_4^\perp} \Big|_{e_4} \right\|_{L_\infty(e_4)} \lesssim \max \left\{ \left| \frac{\partial s}{\partial x}(v_i) \right|, \left| \frac{\partial s}{\partial y}(v_i) \right|, i = 1, 4, h \left| \frac{\partial^2}{\partial e_4 \partial e_4^\perp}(s|_{T_4})(v_1) \right| \right\},$$

which implies, in particular,

$$h \left| \frac{\partial s}{\partial e_4^\perp}(w_4) \right| \lesssim M.$$

Now, by Lemma 3.2 applied to T_3, T_4 , we have $\|s|_{\bar{e}_4}\|_{L_\infty(\bar{e}_4)} \lesssim M$, which, together with (3.9) implies

$$\max \left\{ h \left| \frac{\partial s}{\partial x}(v) \right|, h \left| \frac{\partial s}{\partial y}(v) \right| \right\} \lesssim M.$$

Therefore, by Lemma 3.1, we obtain $\|s\|_{L^\infty(T_1 \cup T_3 \cup T_4)} \lesssim M$. After estimating the normal derivative of s at, say, the midpoint of \bar{e}_2 , we apply Lemma 3.1 on T_2 and thereby complete the proof of (3.7).

The final statement of the lemma follows immediately from the estimates (3.4)–(3.7) and the well-known fact that the space of all C^1 cubic piecewise polynomials with respect to Δ_Q has dimension 16. \square

Proceeding to the computation of the dimension of \mathcal{S}_n , we say that an interior edge of \diamond_n is *strictly interior* if it is also interior with respect to $\diamond_n \setminus \partial\diamond_n$, and denote by $\mathcal{E}_n^{\text{si}}$ the set of all such edges. Furthermore, we denote by \mathcal{V}_n^{i} the set of all interior vertices of \diamond_n .

Theorem 3.4. *The dimension of \mathcal{S}_n is given by the formula*

$$\dim \mathcal{S}_n = 3\#\mathcal{V}_n^{\text{i}} + \#\mathcal{E}_n^{\text{si}}. \quad (3.10)$$

Proof. We denote by w_e the midpoint of an edge e of Δ_n . It suffices to show that the linear functionals

$$\begin{aligned} s(v), \frac{\partial s}{\partial x}(v), \frac{\partial s}{\partial y}(v), \quad v \in \mathcal{V}_n^{\text{i}}, \\ \frac{\partial s}{\partial e^\perp}(w_e), \quad e \in \mathcal{E}_n^{\text{si}}, \end{aligned} \quad (3.11)$$

($s \in \mathcal{S}_n$) form a basis for the dual space \mathcal{S}_n^* . (Indeed, the number of functionals in (3.11) is exactly the number in the right hand side of (3.10).)

To this end, we first show that the functionals (3.11) span \mathcal{S}_n^* . This will follow if for any $s \in \mathcal{S}_n$,

$$s(v) = \frac{\partial s}{\partial x}(v) = \frac{\partial s}{\partial y}(v) = 0, \quad v \in \mathcal{V}_n^{\text{i}}, \quad \frac{\partial s}{\partial e^\perp}(w_e) = 0, \quad e \in \mathcal{E}_n^{\text{si}},$$

implies $s = 0$. By Lemma 3.1, the above assumptions imply that $s|_{Q \cap \bar{\Omega}} = 0$ for any $Q \in \partial\diamond_n$ since the vertex v of Q which belongs to Ω is in \mathcal{V}_n^{i} , and the function and first derivatives of s on the edge $Q \cap \partial\Omega$ are zero because of the boundary conditions. Let now $Q \in \diamond_n \setminus \partial\diamond_n$. Then the function and derivative values of $s|_Q$ listed in (3.4) of Lemma 3.3 are all zero, either by the above assumption (for interior vertices and strictly interior edges), or by boundary conditions (for boundary vertices and edges), or due to the fact that $s|_{Q' \cap \bar{\Omega}} = 0$ for each $Q' \in \partial\diamond_n$ sharing an edge with Q . Therefore, $s|_Q = 0$ by Lemma 3.3.

It remains to show that the functionals (3.11) are linearly independent, or, equivalently, for any real a_v, a_v^x, a_v^y , $v \in \mathcal{V}_n^i$, and $a_e, e \in \mathcal{E}_n^{\text{si}}$, there exists an $s \in \mathcal{S}_n$ such that

$$s(v) = a_v, \quad \frac{\partial s}{\partial x}(v) = a_v^x, \quad \frac{\partial s}{\partial y}(v) = a_v^y, \quad v \in \mathcal{V}_n^i, \quad \frac{\partial s}{\partial e^\perp}(w_e) = a_e, \quad e \in \mathcal{E}_n^{\text{si}}.$$

We start by constructing $s|_{Q \cap \bar{\Omega}}$ for each $Q \in \partial \diamond_n$. Denote by T_1, T_2 the two triangles of Δ_n that make up $Q \cap \bar{\Omega}$, by e their common edge, by e^b the diagonal of Q which is on $\partial \Omega$, by v^b the vertex of e that is on both diagonals of Q , and by v the other vertex of e . We determine $p_1 = s|_{T_1}$ and $p_2 = s|_{T_2}$ by using the interpolation scheme of Lemma 3.1, where v plays the role of v_1 . To check that the two bivariate cubic polynomials p_1, p_2 join with a C^1 smoothness across e , we first observe that $p_1(v^b) = p_2(v^b) = 0$, $\frac{\partial p_1}{\partial e}(v^b) = \frac{\partial p_2}{\partial e}(v^b) = 0$ and $p_1(v) = p_2(v)$, $\frac{\partial p_1}{\partial e}(v) = \frac{\partial p_2}{\partial e}(v)$. This implies that univariate cubic polynomials $p_1|_e$ and $p_2|_e$ coincide. The C^1 -smoothness will follow if we in addition show that $\frac{\partial p_1}{\partial \nu}|_e$ and $\frac{\partial p_2}{\partial \nu}|_e$ also coincide, for some direction ν non-collinear with e . We choose the direction of the edge e^b and notice that $\frac{\partial p_1}{\partial e^b}(v^b) = \frac{\partial p_2}{\partial e^b}(v^b) = 0$ and $\frac{\partial p_1}{\partial e^b}(v) = \frac{\partial p_2}{\partial e^b}(v)$. Moreover, since $\frac{\partial p_1}{\partial e}|_{e^b \cap T_1} = 0$ and $\frac{\partial p_2}{\partial e}|_{e^b \cap T_2} = 0$, it follows that $\frac{\partial^2 p_1}{\partial e^b \partial e}(v^b) = \frac{\partial^2 p_2}{\partial e^b \partial e}(v^b) = 0$. Thus, the univariate quadratic polynomials $\tilde{p}_1(t) := \frac{\partial p_1}{\partial e^b}(tv + (1-t)v^b)$ and $\tilde{p}_2(t) := \frac{\partial p_2}{\partial e^b}(tv + (1-t)v^b)$, $t \in [0, 1]$, satisfy $\tilde{p}_1(0) = \tilde{p}_2(0) = \tilde{p}_1'(0) = \tilde{p}_2'(0) = 0$, $\tilde{p}_1(1) = \tilde{p}_2(1)$ and, hence, coincide, i.e., $\frac{\partial p_1}{\partial e^b}|_e = \frac{\partial p_2}{\partial e^b}|_e$.

Let now $Q \in \diamond_n \setminus \partial \diamond_n$. We construct $s|_Q$ by using (3.4) of Lemma 3.3, where the required function and derivative values on the boundary of Q are given as a_v, a_v^x, a_v^y for a vertex $v \in \mathcal{V}_n^i$, as a_e for an edge $e \in \mathcal{E}_n^{\text{si}}$, as zeros for the vertices and edges on the boundary of Ω . For any edge e that Q shares with a $Q' \in \partial \diamond_n$, the missing normal derivative at the midpoints w_e of e is computed as $\frac{\partial s|_Q}{\partial e^\perp}(w_e) = \frac{\partial s|_{Q'}}{\partial e^\perp}(w_e)$. Lemma 3.3 now guarantees that $s|_Q$ is C^1 -smooth across the diagonals of Q .

Finally, the C^1 -smoothness of s across any interior edge e of \diamond_n follows from the fact that by Condition (e), at least one of both quadrangles at both sides of e is in $\diamond_n \setminus \partial \diamond_n$, and so by construction the two polynomial pieces of s on both triangles attached to e have identical function and first derivative values at the vertices of e , and identical normal derivatives at w_e . \square

4 Stable local Lagrange bases

The dual basis from the proof of Theorem 3.4 provides a local *Hermite-type basis* for the space \mathcal{S}_n . In this section we construct a *Lagrange basis* for the same space, with certain properties required to achieve our goals.

Given $Q \in \diamond_n^\bullet$ with *western* subtriangle T_Q inside $\bar{\Omega}$, i.e., $T_Q \in \Delta_n$, let v_1, v_2, v_3 be the vertices of T_Q in counterclockwise order, with v_1 being the intersection point of the diagonals of Q . We set

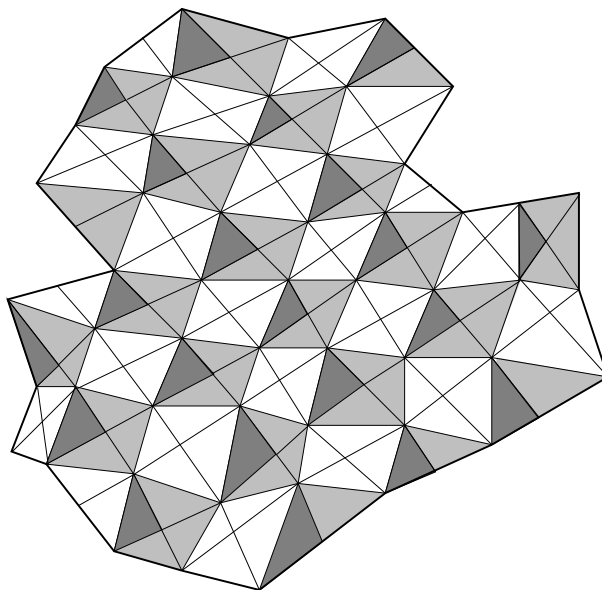


Figure 7: Triangulation Δ_0 , where western subtriangles of $Q \in \diamond_0^\bullet$ are shaded.

$$\begin{aligned}
 D(v_1) &:= \{v_1, \frac{2}{3}v_1 + \frac{1}{3}v_2, \frac{2}{3}v_1 + \frac{1}{3}v_3\}, \\
 D(v_2) &:= \{v_2, \frac{2}{3}v_2 + \frac{1}{3}v_1, \frac{2}{3}v_2 + \frac{1}{3}v_3\}, \\
 D(v_3) &:= \{v_3, \frac{2}{3}v_3 + \frac{1}{3}v_1, \frac{2}{3}v_3 + \frac{1}{3}v_2\}, \\
 D_Q &:= \bigcup \{D(v_k) : k = 2, 3, v_k \notin \partial\Omega\} \\
 c &:= \frac{2}{3}v_1 + \frac{2}{9}v_2 + \frac{1}{9}v_3.
 \end{aligned}$$

For any $Q \in \diamond_n$, let

$$\text{si}(Q)$$

denote the number of edges of Q that are strictly interior, *i.e.*, belong to $\mathcal{E}_n^{\text{si}}$. Clearly, $\text{si}(Q) = 0$ if $Q \in \partial\Diamond_n$. If $\text{si}(Q) = 2$, we denote by w one of the points $w_1 = \frac{2}{3}v_1 + \frac{1}{3}v_2$ and $w_2 = \frac{2}{3}v_1 + \frac{1}{3}v_3$, according to the following rule: If the two strictly interior edges of Q share a vertex v of Q , then w is on the diagonal of Q containing v . Otherwise, two opposite edges of Q are not strictly interior, and it follows by Condition (f) that at least one of them lies on the boundary of Ω . Therefore, there is a diagonal of Q with both endpoints on the boundary of Ω , and we choose w on this diagonal.

We now define the set of points $\Xi_Q \subset T_Q \subset Q$ by

$$\Xi_Q := \begin{cases} D_Q \cup D(v_1) \cup \{c\}, & \text{if } \text{si}(Q) = 4, \\ D_Q \cup D(v_1), & \text{if } \text{si}(Q) = 3, \\ D_Q \cup D(v_1) \setminus \{w\}, & \text{if } \text{si}(Q) = 2, \\ D_Q \cup \{v_1\}, & \text{if } \text{si}(Q) = 1, \\ D_Q, & \text{if } \text{si}(Q) = 0, \end{cases}$$

see Figures 8–12. Finally, defining $\Xi_Q = \emptyset$ when the western subtriangle of $Q \in \Diamond_n^\bullet$ is not in $\bar{\Omega}$, we set

$$\Xi_n := \bigcup_{Q \in \Diamond_n^\bullet} \Xi_Q.$$

Note that 1) the sets Ξ_Q are disjoint for different Q , 2) $\#\Xi_Q = \#D_Q + \text{si}(Q)$, 3) $\#D_Q$ is exactly three times the number of vertices of T_Q that are in \mathcal{V}_n^i , and each $v \in \mathcal{V}_n^i$ is a vertex of T_Q for one and only one $Q \in \Diamond_n^\bullet$, and 4) every strictly interior edge $e \in \mathcal{E}_n^{\text{si}}$ is an edge of one and only one $Q \in \Diamond_n^\bullet$. Therefore,

$$\#\Xi_n = \sum_{Q \in \Diamond_n^\bullet} \#\Xi_Q = \sum_{Q \in \Diamond_n^\bullet} \#D_Q + \text{si}(Q) = 3\#\mathcal{V}_n^i + \#\mathcal{E}_n^{\text{si}} = \dim \mathcal{S}_n,$$

where the last equality sign follows from Theorem 3.4.

For any $Q \in \Diamond_n$, we denote by $\text{star}(Q)$ the union of all quadrilaterals in \Diamond_n having at least one vertex in common with Q , intersected with $\bar{\Omega}$

$$\text{star}(Q) := \bigcup \{Q' \cap \bar{\Omega} : Q' \in \Diamond_n, Q' \cap Q \neq \emptyset\},$$

and by $\text{star}^2(Q)$ the union of stars of the quadrilaterals whose interiors have nonempty intersection with $\text{star}(Q)$,

$$\text{star}^2(Q) := \bigcup \{\text{star}(Q') : Q' \in \Diamond_n, \text{int } Q' \cap \text{star}(Q) \neq \emptyset\}.$$

Theorem 4.1. *The set Ξ_n is a Lagrange interpolation set for \mathcal{S}_n , $n = 0, 1, \dots$, i.e., for any real numbers a_ξ , $\xi \in \Xi_n$, there exists a unique function $s \in \mathcal{S}_n$ such that*

$$s(\xi) = a_\xi, \quad \xi \in \Xi_n.$$

Moreover,

$$\|s\|_{L_\infty(Q \cap \bar{\Omega})} \lesssim \max \{|a_\xi| : \xi \in \Xi_n \cap \text{star}^2(Q)\}, \quad Q \in \diamond_n, \quad (4.1)$$

with a constant depending only on the minimal angle θ .

Proof. The first statement of the theorem is equivalent to the claim that the point evaluation functionals

$$s(\xi), \quad \xi \in \Xi_n,$$

form a basis for the dual space \mathcal{S}_n^* . Since $\#\Xi_n = \dim \mathcal{S}_n$, this claim will follow once we show that these functionals span \mathcal{S}_n^* , i.e., that for any $s \in \mathcal{S}_n$, the condition $s(\xi) = 0$, $\xi \in \Xi_n$, implies $s = 0$. Therefore, both statements of the theorem follow from the inequality

$$\|s\|_{L_\infty(Q \cap \bar{\Omega})} \lesssim \max \{|s(\xi)| : \xi \in \Xi_n \cap \text{star}^2(Q)\}, \quad Q \in \diamond_n, \quad s \in \mathcal{S}_n, \quad (4.2)$$

that we are now going to check.

Let $s \in \mathcal{S}_n$. We will prove (4.2) in several steps.

Step 1. Let $Q \in \partial \diamond_n$. If all three vertices of the triangle $Q \cap \bar{\Omega}$ belong to the boundary of Ω , then $s|_{Q \cap \bar{\Omega}} = 0$ by Lemma 3.1, and (4.2) trivially holds. Otherwise, one of the vertices of $Q \cap \bar{\Omega}$, call it \tilde{v} , is in \mathcal{V}_n^i , and Condition (c) shows that \tilde{v} is a vertex of $T_{Q'}$ for one and only one $Q' \in \diamond_n^\bullet$. In this step, we will prove that

$$\|s\|_{L_\infty(Q \cap \bar{\Omega})} \lesssim \max \{|s(\xi)| : \xi \in \Xi_n \cap T_{Q'}\}, \quad Q \in \partial \diamond_n, \quad (4.3)$$

which obviously implies (4.2) for these Q .

In the notations we used to define $\Xi_{Q'}$, \tilde{v} is either v_2 or v_3 , and in the following we let \bar{v} denote the other of these two vertices, and in accordance with the earlier notation we let v_1 denote the intersection point of the diagonals of Q' . We put $e_1 = [\tilde{v}, v_1]$ and $\bar{e} = [\tilde{v}, \bar{v}]$. Two univariate cubic polynomials $\bar{p}(t) := s(t\bar{v} + (1-t)\tilde{v})$ and $p_1(t) := s(tv_1 + (1-t)\tilde{v})$, $t \in [0, 1]$, will play an essential role below.

Assume first that $Q' = Q$. Then the edge $[\bar{v}, v_1]$ is on the boundary, and hence $s(\bar{v}) = \frac{\partial s}{\partial x}(\bar{v}) = \frac{\partial s}{\partial y}(\bar{v}) = 0$, $s(v_1) = \frac{\partial s}{\partial x}(v_1) = \frac{\partial s}{\partial y}(v_1) = 0$, and $\frac{\partial s}{\partial n}(\frac{\bar{v}+v_1}{2}) = 0$. Since $\tilde{v} \notin \partial\Omega$ and $\text{si}(Q) = 0$, we have $\Xi_Q = \{\tilde{v}, \frac{2}{3}\tilde{v} + \frac{1}{3}\bar{v}, \frac{2}{3}\tilde{v} + \frac{1}{3}v_1\}$. The polynomials \bar{p}, p_1 satisfy the interpolation conditions

$$\begin{aligned} \bar{p}(0) &= s(\tilde{v}), & \bar{p}(\frac{1}{3}) &= s(\frac{2}{3}\tilde{v} + \frac{1}{3}\bar{v}), & \bar{p}(1) &= \bar{p}'(1) = 0, \\ p_1(0) &= s(\tilde{v}), & p_1(\frac{1}{3}) &= s(\frac{2}{3}\tilde{v} + \frac{1}{3}v_1), & p_1(1) &= p_1'(1) = 0. \end{aligned} \quad (4.4)$$

Therefore, the well-posedness of such a cubic interpolation scheme implies that

$$\begin{aligned} |\bar{e}| \left| \frac{\partial s}{\partial \bar{e}}(\tilde{v}) \right| &= |\bar{p}'(0)| \lesssim \max\{|s(\tilde{v})|, |s(\frac{2}{3}\tilde{v} + \frac{1}{3}\bar{v})|\}, \\ |e_1| \left| \frac{\partial s}{\partial e_1}(\tilde{v}) \right| &= |p_1'(0)| \lesssim \max\{|s(\tilde{v})|, |s(\frac{2}{3}\tilde{v} + \frac{1}{3}v_1)|\}, \end{aligned}$$

and so with h being the diameter of T_Q , we conclude that

$$\max \left\{ h \left| \frac{\partial s}{\partial x}(\tilde{v}) \right|, h \left| \frac{\partial s}{\partial y}(\tilde{v}) \right| \right\} \lesssim \max\{|s(\tilde{v})|, |s(\frac{2}{3}\tilde{v} + \frac{1}{3}\bar{v})|, |s(\frac{2}{3}\tilde{v} + \frac{1}{3}v_1)|\},$$

with a constant depending only on the smallest angle in T_Q . Lemma 3.1, applied to T_Q as well as to the triangle $Q \setminus T_Q \cap \bar{\Omega}$, now shows that

$$\|s\|_{L^\infty(Q \cap \bar{\Omega})} \lesssim \max_{\xi \in \Xi_Q} |s(\xi)|,$$

with a constant depending only on the smallest angle θ , which in turn implies (4.3).

Assume now that $Q' \neq Q$. It then follows from Condition (f) that $Q' \in \diamond_n \setminus \partial\diamond_n$. If $\bar{v} \in \partial\Omega$, then the polynomial \bar{p} satisfies (4.4). Otherwise, we use the interpolation scheme

$$\bar{p}(0) = s(\tilde{v}), \quad \bar{p}(\frac{1}{3}) = s(\frac{2}{3}\tilde{v} + \frac{1}{3}\bar{v}), \quad \bar{p}(\frac{2}{3}) = s(\frac{1}{3}\bar{v} + \frac{2}{3}\bar{v}), \quad \bar{p}(1) = s(\bar{v}),$$

and in both cases we arrive at

$$|\bar{e}| \left| \frac{\partial s}{\partial \bar{e}}(\tilde{v}) \right| = |\bar{p}'(0)| \lesssim \max_{\xi \in \Xi_{Q'} \cap \bar{e}} |s(\xi)|. \quad (4.5)$$

Analogously, in case

$$\{\tilde{v}, \frac{2}{3}\tilde{v} + \frac{1}{3}v_1, \frac{1}{3}\tilde{v} + \frac{2}{3}v_1, v_1\} \subset \Xi_{Q'} \cap e_1, \quad (4.6)$$

we get

$$|e_1| \left| \frac{\partial s}{\partial e_1}(\tilde{v}) \right| = |p'_1(0)| \lesssim \max_{\xi \in \Xi_{Q'} \cap e_1} |s(\xi)| \lesssim \max_{\xi \in \Xi_{Q'}} |s(\xi)|. \quad (4.7)$$

With the bounds we derived for $|\frac{\partial s}{\partial \bar{e}}(\tilde{v})|$ and $|\frac{\partial s}{\partial e_1}(\tilde{v})|$, we infer (4.3) similarly to the case that $Q = Q'$.

Condition (f) shows that if Q' only shares \tilde{v} with Q but not an edge, then both edges of Q' emanating from \tilde{v} are strictly interior, and Q' has no common edges with quadrilaterals in $\diamond_n \setminus \partial \diamond_n$. If $\text{si}(Q') \geq 3$, then (4.6) is valid. Otherwise $\text{si}(Q') = 2$, and both edges e' , e'' emanating from the vertex u of Q' opposite to \tilde{v} are on $\partial \Omega$, so that $\Xi_{Q'} = D(\tilde{v}) \cup D(v_1) \setminus \{\frac{2}{3}v_1 + \frac{1}{3}\tilde{v}\}$, and in particular, $\Xi_{Q'} \cap e_1 = \{\tilde{v}, \frac{2}{3}\tilde{v} + \frac{1}{3}v_1, v_1\}$ i.e., (4.6) is *not* valid, and we will derive (4.7) in a different way. With $e_2 := [u, v_1]$, from the fact that on both e' and e'' , s as well as its normal derivative are identically zero, an application of Lemma 3.2 shows that $\|s\|_{L^\infty(e_2)} \lesssim |s(v_1)|$, and so by Markov's inequality we have

$$|e_1| \left| \frac{\partial s}{\partial e_1}(v_1) \right| \approx |e_2| \left| \frac{\partial s}{\partial e_2}(v_1) \right| \lesssim |s(v_1)|.$$

Using the interpolation scheme

$$p_1(0) = s(\tilde{v}), \quad p_1\left(\frac{1}{3}\right) = s\left(\frac{2}{3}\tilde{v} + \frac{1}{3}v_1\right), \quad p_1(1) = s(v_1), \quad p'_1(1) = |e_1| \left| \frac{\partial s}{\partial e_1}(v_1) \right|,$$

we arrive at (4.7).

Now suppose that Q' shares its edge $\bar{e} = [\tilde{v}, \bar{v}]$ with Q . In view of Condition (f), the other edge of Q' emanating from \tilde{v} is strictly interior, and hence $1 \leq \text{si}(Q') \leq 3$. In the case $\text{si}(Q') = 3$ the inclusion (4.6) holds and implies (4.7). Moreover, it is not difficult to see that the same is true if $\text{si}(Q') = 2$. Indeed, if the edge e' of Q' opposite to \bar{e} is strictly interior, then the point w (in the notation we used to define $\Xi_{Q'}$) is on the diagonal containing the common vertex of the two strictly interior edges, hence $w \notin e_1$, which implies (4.6). Otherwise, by Condition (f), e' lies on the boundary of Ω , and w is chosen on the diagonal of Q' with both endpoints on the boundary. Since $\tilde{v} \notin \partial \Omega$, w is not on e_1 in this case either.

It remains to consider the case $\text{si}(Q') = 1$. Then $\Xi_{Q'} \cap e_1 = \{\tilde{v}, \frac{2}{3}\tilde{v} + \frac{1}{3}v_1, v_1\}$. By Condition (f), the edge e' of Q' opposite to the common edge \bar{e} of Q and Q' belongs to the boundary of Ω , which implies that s along with its first normal derivative is zero on e' . As above, we denote by u the vertex of Q' opposite to \tilde{v} , and by e'' the edge of Q' different from e' emanating from u . There are two possibilities for e'' since it is not strictly interior: Either it

also belongs to the boundary, or Q' shares it with a quadrilateral $Q'' \in \partial\mathcal{D}_n$. Since $\bar{v}, u \in \partial\Omega$, in the latter case all three vertices of the triangle $Q'' \cap \bar{\Omega}$ are on $\partial\Omega$, and so $s|_{Q''} = 0$ by Lemma 3.1. We conclude that s and its first order derivatives are zero at both endpoints of e'' and also that its first normal derivative is zero at the midpoint of e'' , meaning that s along with its first order normal derivative vanishes on e'' . Since this obviously also holds when e'' belongs to the boundary, we arrive at same situation that we already encountered in the case $Q \cap Q' = \{\tilde{v}\}$, and that was shown above to imply (4.7) and thus (4.3).

Step 2. We prove that for any $Q \in \mathcal{D}_n^\bullet$ and each vertex v of T_Q ,

$$\max \left\{ |s(v)|, h \left| \frac{\partial s}{\partial x}(v) \right|, h \left| \frac{\partial s}{\partial y}(v) \right| \right\} \lesssim \max \{ |s(\xi)| : \xi \in \Xi_n \cap \text{star}(Q) \}. \quad (4.8)$$

In view of the Markov inequality, it is sufficient to show that for any edge e of T_Q ,

$$\|s\|_{L^\infty(e)} \lesssim \max \{ |s(\xi)| : \xi \in \Xi_n \cap \text{star}(Q) \}. \quad (4.9)$$

Let v_1, v_2, v_3 be the three vertices of T_Q in the notation introduced at the beginning of this section. The edge $[v_2, v_3]$ contains two points of Ξ_n for each of v_2, v_3 not lying on the boundary, and the standard argument involving the appropriate univariate Lagrange or Hermite interpolation scheme shows that (4.9) holds for $e = [v_2, v_3]$.

Let us now consider $e = [v_i, v_1]$ for some $i = 2, 3$, say for $i = 2$. Clearly, if $Q \in \partial\mathcal{D}_n$, then (4.9) follows from (4.3), and so there remains to consider $Q \in \mathcal{D}_n^\bullet \setminus \partial\mathcal{D}_n$.

If $\text{si}(Q) \geq 3$, then e contains four points of Ξ_n if $v_2 \in \mathcal{V}_n^i$, and two points if $v_2 \in \partial\Omega$. In both cases (4.9) immediately follows.

Let $\text{si}(Q) = 2$. We first assume that the two edges e', e'' of Q emanating from v_2 are not strictly interior. If e' is a boundary edge, then s as well as its first order derivatives vanish on e' . Otherwise Q shares e' with a quadrilateral from $\partial\mathcal{D}_n$, and with M being the right hand side of (4.9), (4.3) together with the Markov inequality show that

$$h \left\| \frac{\partial s}{\partial x} \right\|_{L^\infty(e')} \lesssim M, \quad h \left\| \frac{\partial s}{\partial y} \right\|_{L^\infty(e')} \lesssim M, \quad \|s\|_{L^\infty(e')} \lesssim M.$$

The same conclusions are valid for e'' . Since $v_1 \in \Xi_Q$, an application of Lemma 3.2 with T_1, T_2 being the two subtriangles of Q sharing the edge e , now shows that $\|s\|_{L^\infty(e)} \lesssim M$.

If $\text{si}(Q) = 2$ and the above edges e', e'' are strictly interior, then, with $\tilde{e} = [v_1, u]$ where u is the vertex of Q opposite to v_2 , the same arguments show that $\|s\|_{L_\infty(\tilde{e})} \lesssim M$, and so, by Markov's inequality,

$$|e| \left| \frac{\partial s}{\partial e}(v_1) \right| \approx |\tilde{e}| \left| \frac{\partial s}{\partial \tilde{e}}(v_1) \right| \lesssim M,$$

which in turn leads to $\|s\|_{L_\infty(e)} \lesssim M$ by the standard argument.

The remaining cases when $\text{si}(Q) = 2$ and two *opposite* edges of Q are strictly interior, $\text{si}(Q) = 1$ or $\text{si}(Q) = 0$ follow in a similar way from Lemma 3.3 by estimates (3.7), (3.6) or (3.4), respectively.

Step 3. We prove (4.2) for each $Q \in \diamond_n^\bullet \setminus \partial \diamond_n$.

We first assume that $\text{si}(Q) = 4$ and show

$$\|s\|_{L_\infty(T_Q)} \lesssim \max_{\xi \in \Xi_n \cap T_Q} |s(\xi)|. \quad (4.10)$$

Denote by \tilde{T} the *reference triangle* with vertices $\tilde{v}_1 := (0, 0)$, $\tilde{v}_2 := (1, 0)$ and $\tilde{v}_3 := (0, 1)$. Given $Q \in \diamond_n^\bullet$, let $A_Q : \mathbb{R}^2 \rightarrow \mathbb{R}^2$ be the unique affine mapping such that $A_Q(\tilde{v}_i) = v_i$, $i = 1, 2, 3$. Then $A_Q(\tilde{T}) = T_Q$, and for the polynomial $p = s(A_Q \cdot)|_{\tilde{T}} \in \mathcal{P}_3$, we have

$$\|s\|_{L_\infty(T_Q)} = \|p\|_{L_\infty(\tilde{T})}, \quad \max_{\xi \in \Xi_n \cap T_Q} |s(\xi)| = \max_{\xi \in \tilde{\Xi}} |p(\xi)|,$$

where $\tilde{\Xi} := A_Q^{-1}(\Xi_n \cap T_Q)$ is a 10 point set *independent* of $Q \in \diamond_n^\bullet$ and n . Since $\tilde{\Xi}$ consists of 4, ..., 1 points on parallel lines $x + y = 1$, $x + y = 1/3$, $x + y = 2/3$ and $x + y = 0$, respectively, it is a well-posed set for Lagrange interpolation with bivariate cubic polynomials [1]. Therefore,

$$\|p\|_{L_\infty(\tilde{T})} \lesssim \max_{\xi \in \tilde{\Xi}} |p(\xi)|,$$

with an absolute constant. This completes the proof of (4.10). In view of (4.10) and (4.8) (where $\text{star}(Q')$ for some $Q' \subset \text{star}(Q)$ *different* from Q may be involved), a repeated application of Lemma 3.1 starting on a subtriangle T of Q adjacent to T_Q shows (4.2) for such a Q .

Let now $\text{si}(Q) = 3$, and let e be the edge of Q , with midpoint w_e , that fails to be strictly interior. If $e \subset \partial\Omega$ or e is an edge of $\tilde{Q} \in \partial \diamond_n$ such that the triangle $\tilde{Q} \cap \bar{\Omega}$ has all its vertices on $\partial\Omega$, then $\frac{\partial s}{\partial e^\perp}(w_e) = 0$. Otherwise,

e is an edge of $\tilde{Q} \in \partial\Diamond_n$ such that $\tilde{Q} \cap \bar{\Omega}$ has one interior vertex. By noting that this vertex is necessarily also a vertex of Q , an application of (4.3) shows that

$$h \left| \frac{\partial s}{\partial e^\perp}(w_e) \right| \lesssim M,$$

where M denotes the right hand side of (4.2). Because of this estimate and (4.8), a repeated application of Lemma 3.1, starting with the subtriangle of Q attached to e , implies (4.2) for this Q .

Similarly, in the remaining cases where $\text{si}(Q) \leq 2$, (4.2) follows from (4.3) and (4.8) and one of the estimates (3.4), (3.5), (3.6) or (3.7) from Lemma 3.3.

Step 4. We prove (4.2) for each $Q \in \Diamond_n^\circ \setminus \partial\Diamond_n$.

Let v_1, \dots, v_4 be the vertices of Q , and w_1, \dots, w_4 the midpoints of its edges e_1, \dots, e_4 , respectively. Since each v_i is a vertex of $T_{Q'}$ for some $Q' \in \Diamond_n^\bullet$, we have by (4.8),

$$\max \left\{ |s(v_i)|, h \left| \frac{\partial s}{\partial x}(v_i) \right|, h \left| \frac{\partial s}{\partial x}(v_i) \right|, 1 \leq i \leq 4 \right\} \lesssim M,$$

where

$$M = \max \{ |s(\xi)| : \xi \in \Xi_n \cap \text{star}^2(Q) \}.$$

In view of Lemma 3.3, the proof will be completed if we show that

$$h \left| \frac{\partial s}{\partial e_i^\perp}(w_i) \right| \lesssim M \tag{4.11}$$

for each $i = 1, \dots, 4$.

We fix $1 \leq i \leq 4$ and notice that $\frac{\partial s}{\partial e_i^\perp}(w_i) = 0$ if e_i is a boundary edge. Furthermore, if Q shares e_i with a quadrilateral in $\partial\Diamond_n$, then (4.11) follows from (4.3).

It remains to consider the case that e_i is a strictly interior edge. Denote by \tilde{Q} the quadrilateral in $\Diamond_n \setminus \partial\Diamond_n$ such that e_i is a common edge of Q and \tilde{Q} . Obviously, $\tilde{Q} \in \Diamond_n^\bullet$. By (4.8),

$$\max \left\{ |s(v)|, h \left| \frac{\partial s}{\partial x}(v) \right|, h \left| \frac{\partial s}{\partial x}(v) \right| \right\} \lesssim M,$$

for any vertex v of $T_{\tilde{Q}}$. Moreover, in view of (4.3), if e is an edge of \tilde{Q} with vertices u_1, u_2 , and e is not strictly interior, then

$$\max \left\{ |s(u_j)|, h \left| \frac{\partial s}{\partial x}(u_j) \right|, h \left| \frac{\partial s}{\partial x}(u_j) \right|, j = 1, 2, h \left| \frac{\partial s}{\partial e^\perp}\left(\frac{u_1+u_2}{2}\right) \right| \right\} \lesssim M.$$

It is easy to see that the estimates of the last two displays are sufficient for obtaining (4.11) by at most three applications of Lemma 3.1 if $\text{si}(\tilde{Q}) \leq 3$. Finally, if $\text{si}(\tilde{Q}) = 4$, then $h \left| \frac{\partial s}{\partial e^\perp}(w) \right| \lesssim M$ for the midpoint w of each edge e of $T_{\tilde{Q}}$ by (4.10). Now at most two applications of Lemma 3.1 complete the proof of (4.11). \square

The *Lagrange basis functions* B_ξ^n , $\xi \in \Xi_n$, for \mathcal{S}_n are uniquely defined by the conditions

$$B_\xi^n(\eta) = \begin{cases} 1, & \text{if } \eta = \xi, \\ 0, & \text{if } \eta \in \Xi_n \setminus \{\xi\}. \end{cases}$$

By Theorem 4.1, B_ξ^n is well defined, and we have for $\xi \in Q \in \diamond_n^\bullet$,

$$\text{supp } B_\xi^n \subset \text{star}^2(Q),$$

and

$$\|B_\xi^n\|_{L^\infty(\Omega)} \lesssim 1,$$

only depending on θ . Since

$$\text{diam}(Q) \approx 3^{-n}, \quad Q \in \diamond_n, \quad (4.12)$$

only dependent on the initial quadrangulation \diamond_0 , we also have

$$\|B_\xi^n\|_{L_2(\Omega)} \approx 3^{-n}.$$

These properties immediately imply that the bases

$$\{3^n B_\xi^n : \xi \in \Xi_n\}, \quad n = 0, 1, \dots, \quad (4.13)$$

are *uniformly L_2 -stable*, i.e.,

$$\left\| \sum_{\xi \in \Xi_n} c_\xi B_\xi^n \right\|_{L_2(\Omega)} \approx 3^{-n} \left(\sum_{\xi \in \Xi_n} c_\xi^2 \right)^{1/2}, \quad (4.14)$$

for any real numbers c_ξ , where the constants of equivalence are independent of n .

Finally, because of the *triadic* refinement procedure, and our choice of the point c as being $\frac{2}{3}v_1 + \frac{2}{9}v_2 + \frac{1}{9}v_3$ instead of taking the more obvious point $\frac{1}{3}(v_1 + v_2 + v_3)$ as was done in [9], we have

$$\Xi_n \subset \Xi_{n+1}, \quad n = 0, 1, \dots, \quad (4.15)$$

see Figures 8–12.

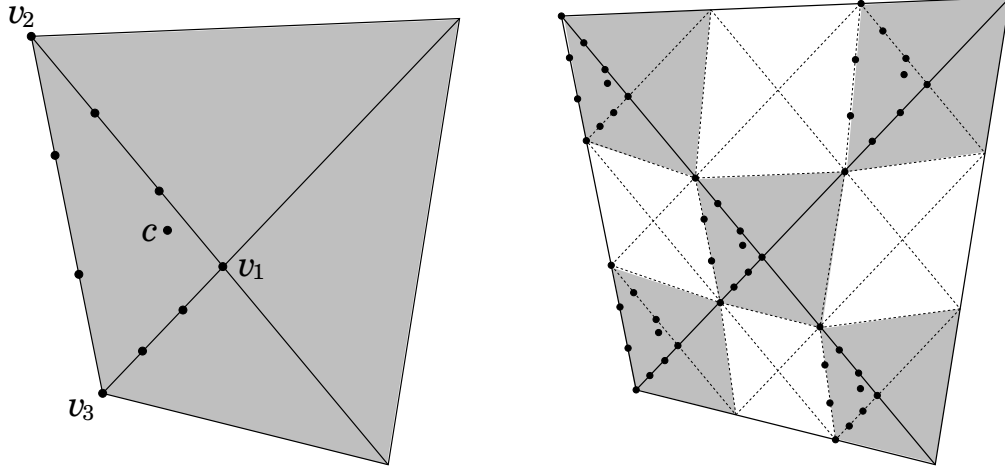


Figure 8: Ξ_Q for some $Q \in \diamond_n^\bullet$ (left) and $\bigcup\{\Xi_{\tilde{Q}} : \tilde{Q} \in \diamond_{n+1}^\bullet, \tilde{Q} \subset Q\}$ (right), in the case $\text{si}(Q) = 4$.

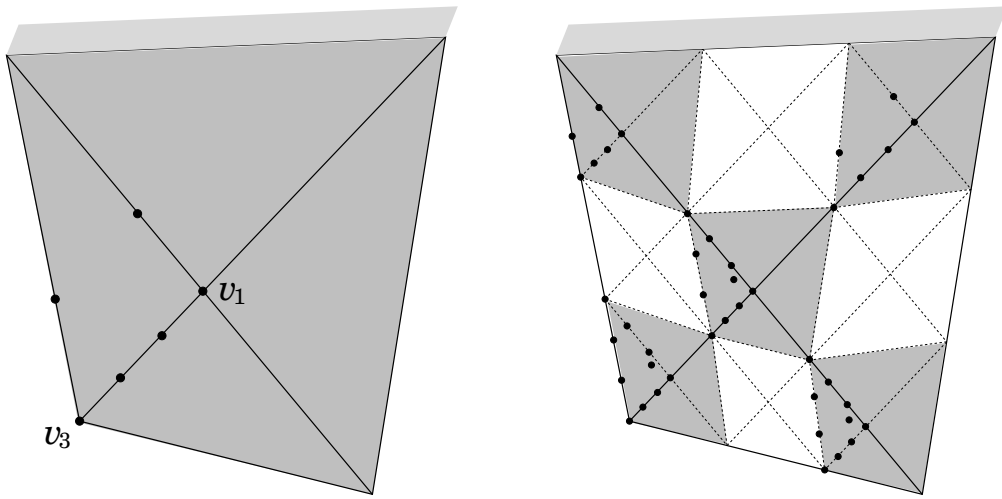


Figure 9: Ξ_Q for some $Q \in \diamond_n^\bullet$ (left) and $\bigcup\{\Xi_{\tilde{Q}} : \tilde{Q} \in \diamond_{n+1}^\bullet, \tilde{Q} \subset Q\}$ (right), in the case $\text{si}(Q) = 3$. Here Q has its northern edge at the boundary. Moreover, $\text{si}(\tilde{Q}) = 3$ for both \tilde{Q} that touch this boundary, and $\text{si}(\tilde{Q}) = 4$ for the other three.

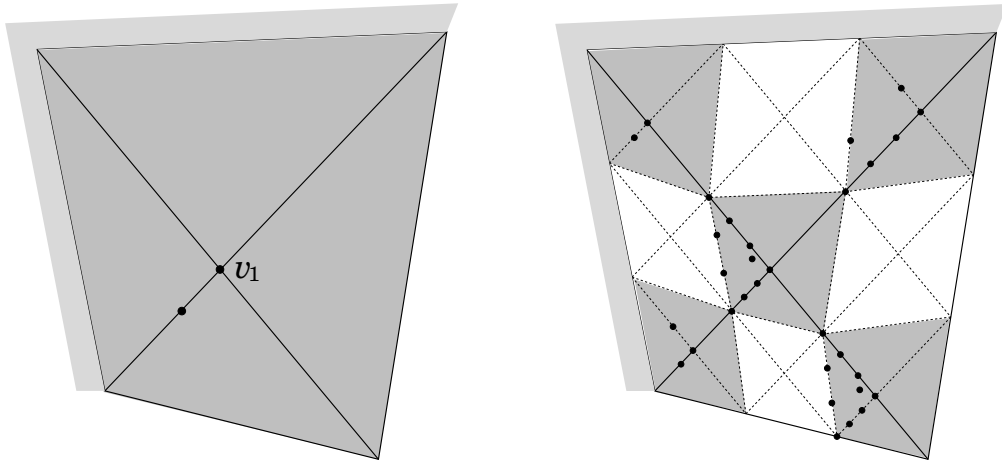


Figure 10: Ξ_Q for some $Q \in \diamond_n^\bullet$ (left) and $\bigcup\{\Xi_{\tilde{Q}} : \tilde{Q} \in \diamond_{n+1}^\bullet, \tilde{Q} \subset Q\}$ (right), in the case $\text{si}(Q) = 2$. Here Q has its northern and western edges at the boundary.

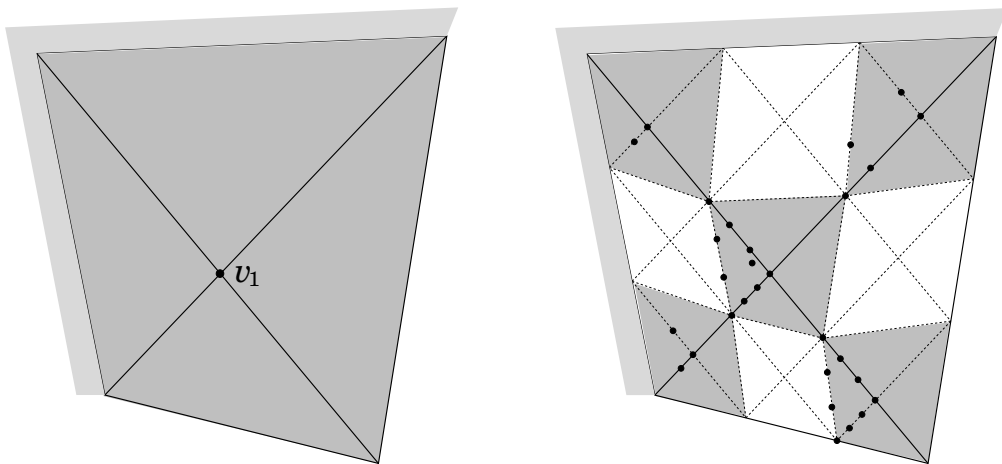


Figure 11: Ξ_Q for some $Q \in \diamond_n^\bullet$ (left) and $\bigcup\{\Xi_{\tilde{Q}} : \tilde{Q} \in \diamond_{n+1}^\bullet, \tilde{Q} \subset Q\}$ (right), in the case $\text{si}(Q) = 1$. Here Q has its northern and western edges at the boundary and shares its eastern edge with a $Q' \in \partial\mathcal{D}_n$. (Q' is not shown.)

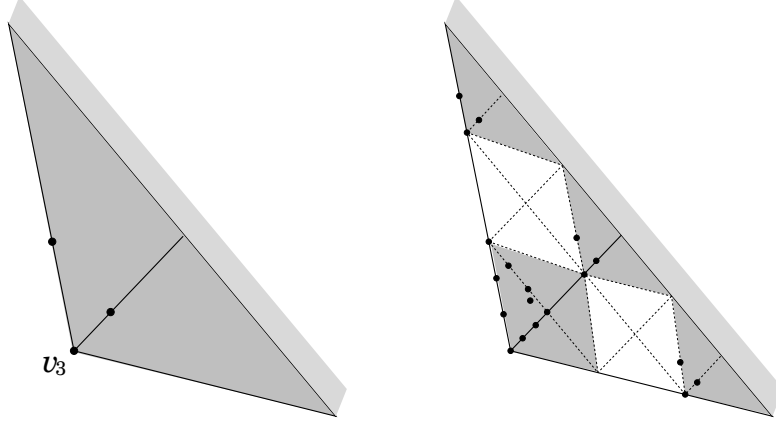


Figure 12: Ξ_Q for some $Q \in \diamond_n^\bullet$ (left) and $\bigcup\{\Xi_{\tilde{Q}} : \tilde{Q} \in \diamond_{n+1}^\bullet, \tilde{Q} \subset Q\}$ (right), in the case $\text{si}(Q) = 0$ and $Q \in \partial\diamond_n$. Only the part $Q \cap \bar{\Omega}$ is shown.

5 Stable multiscale decompositions

Since \mathcal{S}_n has a stable local basis and locally contains all polynomials of degree 3 (with obvious modifications at the boundary), it is easy to see that the following *Jackson estimate*

$$\inf_{u_n \in \mathcal{S}_n} \|u - u_n\|_{L_2(\Omega)} \lesssim 3^{-4n} \|u\|_{H^4(\Omega)} \quad (u \in H^4(\Omega) \cap H_0^2(\Omega))$$

holds (recall (4.12)). On the other hand, since \mathcal{S}_n consists of piecewise polynomials and $\mathcal{S}_n \subset C^1(\bar{\Omega})$, the following *Bernstein estimate* is valid for any $s \in [0, \frac{5}{2})$,

$$\|u_n\|_{H^s(\Omega)} \lesssim 3^{sn} \|u_n\|_{L_2(\Omega)} \quad (u_n \in \mathcal{S}_n).$$

Let us now define $\mathcal{H}^s = [L_2(\Omega), H_0^2(\Omega) \cap H^4(\Omega)]_{s/4}$ for $s \in [0, 4]$, and $\mathcal{H}^s = (\mathcal{H}^{-s})'$ for $s \in [-4, 0)$. Note that $\mathcal{H}^s = H^s(\Omega) \cap H_0^2(\Omega)$ when $s \in [2, 4]$, whereas $\mathcal{H}^s = H_0^s(\Omega)$ when $s \in [0, 2] \setminus \{\frac{1}{2}, \frac{3}{2}\}$ (see [14]).

With Q_n being the $L_2(\Omega)$ -orthogonal projector onto \mathcal{S}_n , and $Q_{-1} := 0$, it is known that as a consequence of the Jackson and Bernstein estimates and the nestedness (2.1) of the spaces \mathcal{S}_n as function of n , it holds that for $|s| < \frac{5}{2}$,

$$\|u\|_{\mathcal{H}^s}^2 \approx \sum_{n=0}^{\infty} 3^{2ns} \|(Q_n - Q_{n-1})u\|_{L_2(\Omega)}^2 \quad (u \in \mathcal{H}^s) \quad (5.1)$$

(see [21, 23, 16, 4]; a relatively short, self-contained proof in the more general biorthogonal setting can be found in [8, Appendix]).

As shown in [11, Proposition 3], a consequence of (5.1) is that for any $s \in (0, \frac{5}{2})$,

$$\|u\|_{\mathcal{H}^s}^2 \approx \inf_{u_n \in \mathcal{S}_n: u = \sum_n u_n} \sum_{n=0}^{\infty} 3^{2ns} \|u_n\|_{L_2(\Omega)}^2 \quad (u \in \mathcal{H}^s), \quad (5.2)$$

where thus the infimum is taken over all representations of u in the form $u = \sum_{n=0}^{\infty} u_n$, $u_n \in \mathcal{S}_n$.

Let \mathcal{I}_n be the Lagrange interpolator onto \mathcal{S}_n corresponding to Theorem 4.1, and let $\mathcal{I}_{-1} := 0$. By the Sobolev embedding theorem, \mathcal{I}_n is well defined on $H^s(\Omega)$ when $s > 1$. As follows from (4.14), for $u_n \in \mathcal{S}_n$ we have

$$\|u_n\|_{L_2(\Omega)} \lesssim 3^{-n} \left(\sum_{\xi \in \Xi_n} u_n(\xi)^2 \right)^{1/2}. \quad (5.3)$$

On the other hand, since \mathcal{S}_m consists of piecewise polynomials, for all $u_m \in \mathcal{S}_m$, $\xi \in \Omega$ and any $T_\xi \in \Delta_m$ containing ξ it holds that

$$|u_m(\xi)| \leq \|u_m\|_{L_\infty(T_\xi)} \approx 3^m \|u_m\|_{L_2(T_\xi)}. \quad (5.4)$$

Therefore, by (5.3),

$$\|\mathcal{I}_n u_m\|_{L_2(\Omega)}^2 \lesssim 3^{-2n} \sum_{\xi \in \Xi_n} |u_m(\xi)|^2 \lesssim 3^{2m-2n} \sum_{\xi \in \Xi_n} \|u_m\|_{L_2(T_\xi)}^2.$$

If $m \geq n$, then every triangle $T \in \Delta_m$ appears in the last sum at most 10 times, so that

$$\sum_{\xi \in \Xi_n} \|u_m\|_{L_2(T_\xi)}^2 = \sum_{\xi \in \Xi_n} \int_{T_\xi} |u_m|^2 \leq 10 \sum_{T \in \Delta_m} \int_T |u_m|^2 = 10 \|u_m\|_{L_2(\Omega)}^2,$$

and we conclude that

$$\|\mathcal{I}_n u_m\|_{L_2(\Omega)} \lesssim 3^{m-n} \|u_m\|_{L_2(\Omega)}, \quad u_m \in \mathcal{S}_m, \quad m \geq n. \quad (5.5)$$

Remark 5.1. By using the nesting (4.15) of the Lagrange interpolation sets, (5.5) can be directly deduced from (4.14) since

$$\sum_{\xi \in \Xi_n} |u_m(\xi)|^2 \leq \sum_{\xi \in \Xi_m} |u_m(\xi)|^2$$

in that case. For completeness we included the above arguments showing that the nesting is not essential at this point.

As a consequence of (5.2) and (5.5), for $s \in (1, \frac{5}{2})$ it holds that

$$\|u\|_{\mathcal{H}^s}^2 \approx \sum_{n=0}^{\infty} 3^{2ns} \|(\mathcal{I}_n - \mathcal{I}_{n-1})u\|_{L_2(\Omega)}^2 \quad (u \in \mathcal{H}^s). \quad (5.6)$$

Although this statement can be deduced from [5], for convenience of the reader we include a short proof here. In view of (5.2), it is sufficient to show the inequality “ \gtrsim ”. For some $s \in (1, \frac{5}{2})$ and $u \in \mathcal{H}^s$, let $u = \sum_{\ell=0}^{\infty} u_{\ell}$ with $u_{\ell} \in \mathcal{S}_{\ell}$. Since the interpolators \mathcal{I}_n are projectors and the spaces \mathcal{S}_n are nested, we have $(\mathcal{I}_n - \mathcal{I}_{n-1})\mathcal{S}_{\ell} = 0$ when $\ell \leq n-1$. From this and (5.5), we have

$$\begin{aligned} & \sum_{n=0}^{\infty} 3^{2ns} \|(\mathcal{I}_n - \mathcal{I}_{n-1})u\|_{L_2(\Omega)}^2 \\ &= \sum_{n=0}^{\infty} \sum_{\ell, \ell'=0}^{\infty} 3^{2ns} ((\mathcal{I}_n - \mathcal{I}_{n-1})u_{\ell}, (\mathcal{I}_n - \mathcal{I}_{n-1})u_{\ell'})_{L_2(\Omega)} \\ &= \sum_{\ell, \ell'=0}^{\infty} \sum_{n=0}^{\min\{\ell, \ell'\}} 3^{2ns} ((\mathcal{I}_n - \mathcal{I}_{n-1})u_{\ell}, (\mathcal{I}_n - \mathcal{I}_{n-1})u_{\ell'})_{L_2(\Omega)} \\ &\lesssim \sum_{\ell, \ell'=0}^{\infty} \sum_{n=0}^{\min\{\ell, \ell'\}} 3^{2ns} 3^{\ell+\ell'-2n} \|u_{\ell}\|_{L_2(\Omega)} \|u_{\ell'}\|_{L_2(\Omega)} \\ &\approx \sum_{\ell, \ell'=0}^{\infty} 3^{(s-1)(2\min\{\ell, \ell'\}-\ell-\ell')} (3^{\ell s} \|u_{\ell}\|_{L_2(\Omega)}) (3^{\ell' s} \|u_{\ell'}\|_{L_2(\Omega)}) \\ &\lesssim \sum_{\ell=0}^{\infty} 3^{2\ell s} \|u_{\ell}\|_{L_2(\Omega)}^2, \end{aligned}$$

where the last line is a consequence of the fact that the infinite matrix $[3^{(s-1)(2\min\{\ell, \ell'\}-\ell-\ell')}]_{\ell', \ell \in \mathbb{N}_0}$ defines a bounded mapping on ℓ_2 . Since the splitting $u = \sum_{\ell=0}^{\infty} u_{\ell}$ was arbitrary, from (5.2) we conclude that

$$\sum_{n=0}^{\infty} 3^{2ns} \|(\mathcal{I}_n - \mathcal{I}_{n-1})u\|_{L_2(\Omega)}^2 \lesssim \|u\|_{\mathcal{H}^s}^2$$

and so that (5.6) is valid.

6 Hierarchical basis and its applications

Thanks to the nesting (4.15) of the interpolation sets, the following subsets of (4.13),

$$\{3^n B_\xi^n : \xi \in \Xi_n \setminus \Xi_{n-1}\}, \quad n = 0, 1, \dots, \quad (\Xi_{-1} := \emptyset),$$

are uniformly L_2 -stable bases for the spaces $\text{Im}(\mathcal{I}_n - \mathcal{I}_{n-1})$. From (5.6) we therefore conclude that for any $s \in (1, \frac{5}{2})$,

$$\cup_{n=0}^{\infty} \{3^{(1-s)n} B_\xi^n : \xi \in \Xi_n \setminus \Xi_{n-1}\} \quad (6.1)$$

is a Riesz basis for \mathcal{H}^s , i.e.,

$$\left\| \sum_{n=0}^{\infty} 3^{(1-s)n} \sum_{\xi \in \Xi_n \setminus \Xi_{n-1}} c_\xi B_\xi \right\|_{H^s(\Omega)}^2 \approx \sum_{n=0}^{\infty} \sum_{\xi \in \Xi_n \setminus \Xi_{n-1}} c_\xi^2.$$

As a consequence, for any $J \in \mathbb{N}$, $\cup_{n=0}^J \{3^{(1-s)n} B_\xi^n : \xi \in \Xi_n \setminus \Xi_{n-1}\}$ is a uniformly \mathcal{H}^s -stable basis for \mathcal{S}_J .

Since for $J \geq 1$, it is the union of the corresponding basis for \mathcal{S}_{J-1} and some complement set, such a basis and also (6.1) are known as *hierarchical bases*.

Remark 6.1. By straightforward adaptation of the proof from §5, for $s = 1$ we obtain the suboptimal result

$$J^{-2} \sum_{n=0}^J \sum_{\xi \in \Xi_n \setminus \Xi_{n-1}} c_\xi^2 \lesssim \left\| \sum_{n=0}^J \sum_{\xi \in \Xi_n \setminus \Xi_{n-1}} c_\xi B_\xi \right\|_{H^1(\Omega)}^2 \lesssim \sum_{n=0}^J \sum_{\xi \in \Xi_n \setminus \Xi_{n-1}} c_\xi^2$$

for any scalars c_ξ .

Remark 6.2. C^1 hierarchical bases were constructed earlier in [5]. There the functionals defining the bases involve both function values and derivatives, so that the corresponding interpolator $\tilde{\mathcal{I}}_n$ is only well defined on $H^s(\Omega)$ when $s > 2$, whereas instead of (5.5), only $\|\tilde{\mathcal{I}}_n u_m\|_{L_2(\Omega)} \lesssim (\rho^{m-n})^2 \|u_m\|_{L_2(\Omega)}$ is valid, with ρ being the refinement factor ($\rho = 2$ in [5] and $\rho = 3$ here). As a consequence, properly scaled, these bases generate Riesz bases for \mathcal{H}^s for $2 < s < \frac{5}{2}$, whereas for the interesting case $s = 2$ a suboptimal result is valid, similar as in Remark 6.1.

The above constructed hierarchical bases can be used to solve the boundary value problems of fourth order. For example, consider the biharmonic equation

$$\Delta^2 u = f \text{ on } \Omega, \quad u = \partial_{\mathbf{n}} u = 0 \text{ on } \partial\Omega,$$

which appears as result of the modeling of plate bending problems. After switching to a variational formulation, the Ritz-Galerkin approximation $u_J \in \mathcal{S}_J$ solves

$$a(u_J, v_J) = (f, v_J)_{L_2(\Omega)} \quad (v_J \in \mathcal{S}_J),$$

where $a(u, v) = \int_{\Omega} \sum_{i,j} \partial_{ij}^2 u \partial_{ij}^2 v \, dx$.

Since $a(v, v) \approx \|v\|_{H^2(\Omega)}^2$ ($v \in H_0^2(\Omega)$), exploiting the properly scaled hierarchical basis $\cup_{n=0}^J \{3^{-n} B_{\xi}^n : \xi \in \Xi_n \setminus \Xi_{n-1}\}$ leads to uniformly well-conditioned stiffness matrices, meaning that standard iterative methods, like the conjugate gradient method, converge with a rate less than 1 uniformly in J . For comparison, note that standard, single scale bases for \mathcal{S}_J give rise to stiffness matrices with condition numbers of the order h_J^{-4} with $h_J = 3^{-J}$.

A potential problem with the use of the hierarchical basis is that, due to the increasing sizes of the supports of the basis functions on lower levels, the resulting stiffness matrix is not (fully) sparse. Indeed, one may verify that this matrix has $\sim \dim \mathcal{S}_J \log(\dim \mathcal{S}_J)$ non-zero entries. Fortunately, a direct matrix-vector multiplication using this matrix can be avoided. Indeed, let Φ_J be a locally supported single-scale basis for \mathcal{S}_J , e.g., the Hermite type basis associated to (3.11). With \mathbf{B}_J , \mathbf{A}_J denoting the stiffness matrices with respect to our hierarchical basis and Φ_J , respectively, and with \mathbf{T}_J denoting the basis transformation from the hierarchical basis to Φ_J , it holds that $\mathbf{B}_J = \mathbf{T}_J^* \mathbf{A}_J \mathbf{T}_J$. The matrix \mathbf{A}_J is sparse, and since by a recursive evaluation, both \mathbf{T}_J and \mathbf{T}_J^* can be performed in $\mathcal{O}(\dim \mathcal{S}_J)$ operations (for details see e.g. [8, §4.4]), we conclude that in this factorized way, \mathbf{B}_J can be applied to a vector taking only $\mathcal{O}(\dim \mathcal{S}_J)$ operations. Similar remarks apply to an efficient evaluation of the right hand side of the matrix-vector system.

Remark 6.3. Under similar assumptions on the triangulations, more general spaces

$$\begin{aligned} \mathcal{S}_n = & \{s \in C^1(\Omega) : s|_T \in \mathcal{P}_3 \text{ for all } T \in \Delta_n, \\ & s = \frac{\partial s}{\partial x} = \frac{\partial s}{\partial y} = 0 \text{ on } \Gamma_0 \subset \partial\Omega, \quad s = 0 \text{ on } \Gamma_1 \subset \partial\Omega\}, \end{aligned}$$

useful for other plate problems commonly encountered in practice (see, e.g. [3]), may also be considered when Γ_0 and Γ_1 are unions of subsets of the edges of

the initial triangulation. (It is possible that Γ_0 or Γ_1 are given in the form of cracks as explained in Remark 2.3.) We conjecture that all the above results extend to these spaces, with natural modifications.

Another application of hierarchical bases is surface compression, see [12]. For this application, the fact that our basis is of Lagrange type, instead of the Hermite basis as employed in [12], has the obvious practical advantage that only Lagrange data of the surface is needed. Also the larger range of stability of our basis might extend its applicability here.

A Construction of an initial quadrangulation

A.1 Convex domains

Let Ω be a convex domain with piecewise linear boundary with vertices v_1, \dots, v_N , $N \geq 3$, in, say, counterclockwise order. It is quite easy to construct an initial quadrangulation satisfying (a)–(e) for such a domain. If $N = 4$, the domain itself is a nondegenerate convex quadrilateral Q , and we take $\diamond_0 = \{Q\}$. For $N = 3$ we define Q as a parallelogram whose three vertices are v_1, v_2, v_3 , and one of diagonals is, say, $[v_1, v_2]$. We again take $\diamond_0 = \{Q\}$. If $N \geq 5$, we split the domain into $\lceil N/2 \rceil - 1$ subdomains by connecting v_i with v_{N-i+1} , $i = 2, \dots, \lceil N/2 \rceil - 1$. If N is even, all subdomains are nondegenerate convex quadrilaterals, and, since they are connected into one strip, it is obvious that Conditions (a)–(e) are satisfied for the quadrangulation they build. If N is odd, we get $\lceil N/2 \rceil - 2$ quadrilaterals and one triangle with vertices $v_{\lceil N/2 \rceil - 1}, v_{\lceil N/2 \rceil}, v_{\lceil N/2 \rceil + 1}$. By extending this last triangle to a parallelogram with these three vertices and diagonal $[v_{\lceil N/2 \rceil - 1}, v_{\lceil N/2 \rceil}]$, we arrive at a quadrangulation satisfying (a)–(e).

Obviously, the introduction of additional subdivisions and properly located interior vertices may improve the quality of this quadrangulation and that of the corresponding starting triangulation Δ_0 .

A.2 Construction of a quadrangulation satisfying (a)–(e) in general

Theorem A.1. *Let Ω be a domain with Lipschitz' continuous, piecewise linear boundary. Then there exists a quadrangulation \diamond_0 satisfying (a)–(e) with respect to Ω .*

Proof. The boundary of Ω is determined by a number of points and an equal number of line segments connecting them. In this construction, we refer to these points as being “nodes”, to distinguish them from the corner points of the polygons in the subdivision of Ω which we call “vertices”. (Thus, all nodes are vertices, but not otherwise.)

For any node v that corresponds to a re-entrant corner with both legs either in the upper or lower half plane, we cut Ω along the *vertical* line ℓ through v . More precisely, if $\Omega \cap \ell$ consists of more than one disjoint parts, we cut Ω only along those parts that either have both v as an endpoint and lie in the other half plane than the legs, or that do not cut Ω in two disconnected parts. By rotating Ω in advance, we may assume that ℓ does not contain nodes other than v .

Let A denote the set of all points of intersection of $\partial\Omega$ and the vertical lines we have drawn, together with all nodes, except those that do both not correspond to a re-entrant corner and have both legs in the same upper or lower half plane. For any $v \in A$, we cut Ω along the *horizontal* line ℓ through v . More precisely, if $\Omega \cap \ell$ consists of more than one disjoint parts, we cut Ω only along those parts that either have v as an endpoint, or that do not cut Ω in two disconnected parts. For an illustration, see Figure 13.

By construction we obtained a subdivision of Ω into polygons. This subdivision is conforming, in the sense that the intersection between any two different polygons in the subdivision is either empty or a common vertex or edge. The number of interior edges emanating from any boundary vertex does not exceed four, and vertices inside Ω are of degree exactly four.

Now suppose that some polygon in the subdivision has three vertices $v^{(1)}, v^{(2)}, v^{(3)}$ with different second coordinates, say $v_y^{(1)} < v_y^{(2)} < v_y^{(3)}$. Since by construction Ω is cut along the horizontal line through $v^{(2)}$ we encounter a contradiction. We conclude that all polygons in the subdivision are either quadrilaterals or triangles.

The (interior) angles at all interior vertices of the subdivision are equal to $\pi/2$, which in particular means that polygons that do not touch the boundary

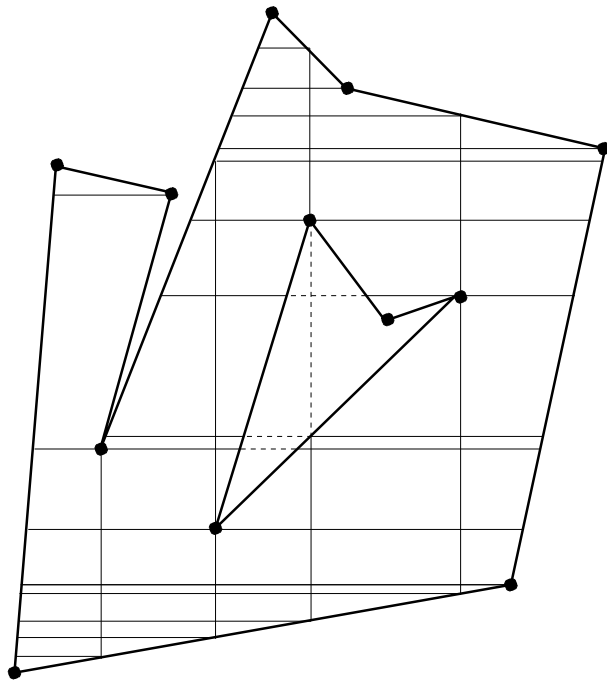


Figure 13: Initial quadrangulation according to the proof of Theorem A.1.

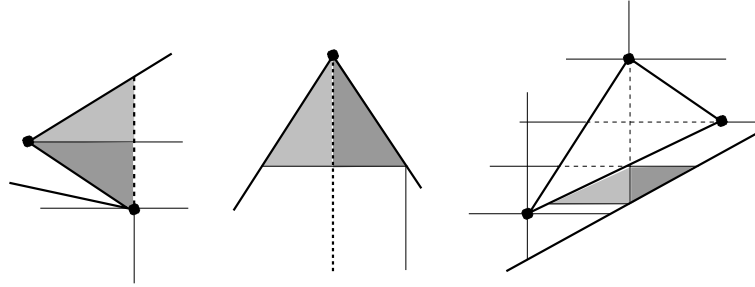


Figure 14: Illustration with Condition (e).

are rectangles. The (interior) angles at vertices on the boundary are $< \pi$ and so all remaining quadrilaterals are also convex.

All drawn horizontal and vertical lines define a logically rectangular mesh put over Ω . Obviously, there exists a black-and-white coloring of the rectangles in this mesh such that each one shares its interior edges only with rectangles of opposite color. Furthermore, there exists a canonical way to assign predicates north, east, south and west to all interior edges of all rectangles such that different rectangles may only share north-south or east-west edges. The polygons from our subdivision are either rectangles of this mesh or they are subsets of such rectangles. Although it may happen that more than one polygons are subsets of one ‘parent’ rectangle, in that case these polygons do not share an edge. We conclude that if we let the polygons inherit both the colors and the predicates north, east, south or west for their internal edges from their parent rectangles, then Condition (c) of Section 2 is satisfied.

For each triangle T from the subdivision, it is easy to construct a quadrilateral Q such that T is equal to $\overline{\Omega} \cap Q$, which in turn is equal to one of both triangles generated by splitting Q along its diagonals. We conclude that our subdivision satisfies (a)–(d).

Finally, we have to check (e). By our use of horizontal and vertical lines only, (e) can only be violated in the three geometrical situations as illustrated in Figure 14. The situations in the left and middle picture can actually not occur, since by construction Ω is not cut along the dotted lines. Yet, the situation in the right picture is possible. However, after one triadic (or dyadic) refinement step as discussed in Section 2, such a situation is no longer

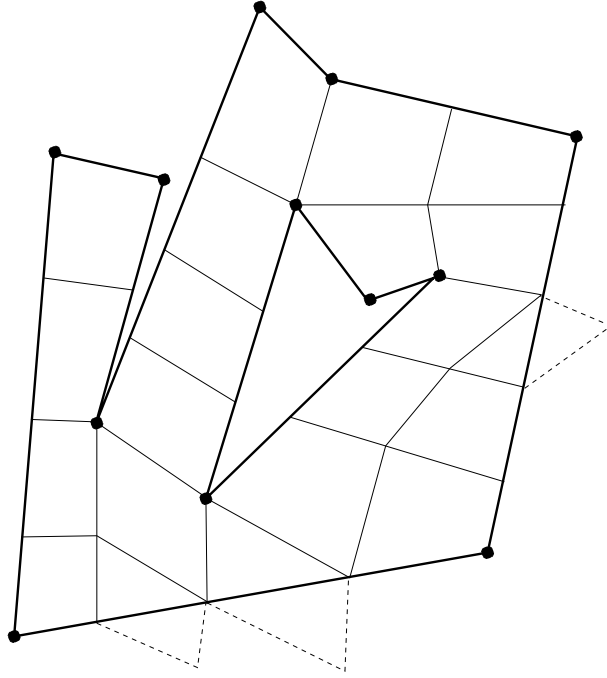


Figure 15: Initial quadrangulation “by hand” for the domain of Figure 13.

possible, so by replacing \diamond_0 by \diamond_1 we have found an initial quadrangulation that satisfies (a)-(e). \square

Remark A.1. Although for simplicity we restricted ourselves to domains with Lipschitz’ continuous boundaries, the construction from the above proof can be extended to domains with cracks.

Remark A.2. Although the construction from the above existence proof may give some hints how to obtain a quadrangulation in practice, it should not be applied without care. Indeed, because of the restriction to horizontal and vertical lines only, even for “nice” domains it may result in quadrilaterals with bad aspect ratios, and small angles. If a given domain is not very complicated, a suitable starting quadrangulation can in many cases be easily found “by hand,” as Figure 15 illustrates.

References

- [1] K. C. Chung and T. H. Yao, On lattices admitting unique Lagrange interpolation, *SIAM J. Num. Anal.*, 14 (1977), 735–743.
- [2] P. G. Ciarlet. *The finite element method for elliptic problems*. North-Holland, The Netherlands, 1978.
- [3] P. G. Ciarlet. *Mathematical elasticity II: Lower-dimensional theories of plates and rods*. North-Holland, The Netherlands, 1990.
- [4] W. Dahmen. Stability of multiscale transformations. *J. Fourier Anal. Appl.*, 4:341–362, 1996.
- [5] W. Dahmen, P. Oswald, and X.-Q. Shi, C^1 -hierarchical bases, *J. Comput. Appl. Math.*, 51 (1994), pp. 37–56.
- [6] W. Dahmen and R. Schneider. Composite wavelet bases for operator equations. *Math. Comp.*, 68:1533–1567, 1999.
- [7] W. Dahmen and R. Schneider, Wavelets on manifolds I: Construction and domain decomposition, *SIAM J. Math. Anal.*, 31 (1999), 184–230.
- [8] W. Dahmen and R.P. Stevenson. Element-by-element construction of wavelets satisfying stability and moment conditions. *SIAM J. Numer. Anal.*, 37(1):319–352, 1999.
- [9] O. Davydov and F. Zeilfelder, Scattered data fitting by direct extension of local polynomials to bivariate splines, *Adv. Comput. Math.*, 21 (2004), 223–271.
- [10] O. Davydov, G. Nürnberger and F. Zeilfelder, Bivariate spline interpolation with optimal approximation order, *Constr. Approx.*, 17 (2001), 181–208.
- [11] M. Griebel and P. Oswald. Tensor product type subspace splittings and multilevel iterative methods for anisotropic problems. *Adv. Comput. Math.*, 4(1–2):171–206, 1995.
- [12] D. Hong and L.L. Schumaker. Surface compression using a space of C^1 cubic splines with a hierarchical basis, *Computing*, 72 (2004), 79–92.

- [13] M.-J. Lai and L. L. Schumaker, On the approximation power of splines on triangulated quadrangulations, *SIAM J. Numer. Anal.*, 36(1) (1999), pp. 143–159.
- [14] J.L. Lions and E. Magenes. *Non-homogeneous boundary value problems and applications. Vol I.* Springer, Berlin, 1972.
- [15] R. Lorentz and P. Oswald, Multilevel finite element Riesz bases for Sobolev spaces. In *Proc. 9th Intern. Conf. on Domain Decomposition Methods in Science and Engineering (P. Bjorstad et al., eds.)*, pages 178–187, Domain Decomposition Press, Bergen, 1998.
- [16] Y. Meyer. *Ondelettes et Operateurs.* Hermann, Paris, 1990.
- [17] J. Morgan and R. Scott, A nodal basis for C^1 piecewise polynomials of degree $n \geq 5$, *Math. Comp.*, 29 (1975), 736–740.
- [18] G. Nürnberger, L. L. Schumaker, F. Zeilfelder, Local Lagrange interpolation by bivariate C^1 cubic splines, in *Mathematical Methods for Curves and Surfaces III: Oslo 2000*, T. Lyche and L. L. Schumaker (eds), Vanderbilt University Press, 2001, 393–404.
- [19] G. Nürnberger, L. L. Schumaker, F. Zeilfelder, Lagrange interpolation by C^1 cubic splines on triangulations of separable quadrangulations, in *Approximation Theory X: Splines, Wavelets, and Applications*, C.K. Chui, T. Lyche and L. L. Schumaker (eds), Vanderbilt University Press, 2002, 405–424.
- [20] G. Nürnberger, L. L. Schumaker, F. Zeilfelder, Lagrange interpolation by C^1 cubic splines on triangulated quadrangulations, *Adv. Comput. Math.*, 21 (2004), 357–380.
- [21] P. Oswald. On discrete norm estimates related to multilevel preconditioners in the finite element method. In *Constructive Theory of Functions, Proc. Int. Conf. Varna 1991, Sofia*, pages 203–214. Bulg. Acad. Sci., 1992.
- [22] P. Oswald. Hierarchical conforming finite element methods for the bi-harmonic equation, *SIAM J. Numer. Anal.*, 29 (1992), 1610–1625.

- [23] P. Oswald. *Multilevel finite element approximation: Theory and applications*. B.G. Teubner, Stuttgart, 1994.
- [24] H. Yserentant. On the multilevel splitting of finite element spaces, *Numer. Math.*, 49 (1986), 379–412.

Oleg Davydov
Department of Mathematics
University of Strathclyde
26 Richmond Street
Glasgow G1 1XH, Scotland, UK
oleg.davydov@strath.ac.uk

Rob Stevenson
Department of Mathematics
Utrecht University
P.O. Box 80.010
3508 TA Utrecht, The Netherlands
stevenso@math.uu.nl